Characterization of chlorinated solvent contamination in limestone using innovative FLUTe® technologies in combination with other methods in a line of evidence approach

Broholm, Mette Martina; Janniche, Gry Sander; Mosthaf, Klaus; Fjordbøge, Annika Sidelmann; Binning, Philip John; Christensen, Anders G.; Grosen, Bernt; Jørgensen, Torben H.; Keller, Carl; Wealthall, Gary; Kerrn-Jespersen, Henriette

Published in:
Journal of Contaminant Hydrology

Link to article, DOI:
10.1016/j.jconhyd.2016.03.007

Publication date:
2016

Document Version
Peer reviewed version

This is a Post Print of the article published online April 6th, 2016 in Journal of Contaminant Hydrology 189 (2016) 68–85. The publishers' version is available at the permanent link: http://dx.doi.org/10.1016/j.jconhyd.2016.03.007

Characterization of Chlorinated Solvent Contamination in Limestone Using Innovative FLUTe® Technologies in Combination with Other Methods in a Line of Evidence Approach

Mette M. Broholm[1], Gry S. Janniche[1], Klaus Mosthaf[1], Annika S. Fjordbøge[1], Philip J. Binning[1], Anders G. Christensen[2], Bernt Grosen[3], Torben H. Jørgensen[3], Carl Keller[4], Gary Wealthall[5], and Henriette Kerrn-Jespersen[6]*

1: DTU Environment, Technical University of Denmark, Kgs. Lyngby, Denmark; 2: NIRAS, Allerød, Denmark; 3: COWI, Kgs. Lyngby, Denmark; 4: FLUTe Technology, 5: GeoSyntec Consultants, Guelph, Ontario, Canada; 6: Capital Region of Denmark, Hillerød, Denmark

Highlights

The determination of DNAPL source zone architecture was improved by combining innovative field methods in a line of evidence approach.

FACT™ provided detailed information on the vertical distribution of chlorinated solvents in a limestone aquifer.

Modelling combined with AC sorption experiments enabled interpretation of FACT™ combined with FLUTe® transmissivity data.

Water FLUTe™ sampling under 2 flow conditions and FACT™ sampling and analysis provided important information regarding potential DNAPL presence.

Abstract

Characterization of dense non-aqueous phase liquid (DNAPL) source zones in limestone aquifers/bedrock is essential to develop accurate site-specific conceptual models and perform risk assessment. Here innovative field methods were combined to improve determination of source zone architecture, hydrogeology and contaminant distribution. The FACT™ is a new technology and it was applied and tested at a contaminated site with a limestone aquifer, together with a number of existing methods including wire-line coring with core subsampling, FLUTe® transmissivity profiling and multilevel water sampling. Laboratory sorption studies were combined with a model of contaminant uptake on the FACT™ for data interpretation. Limestone aquifers were found particularly difficult to sample with existing methods because of core loss, particularly from soft zones in contact with chert beds. Water FLUTe™ multilevel groundwater sampling (under two flow conditions) and FACT™ sampling and analysis combined with FLUTe® transmissivity profiling and modelling were used to provide a line of evidence for the presence of DNAPL, dissolved and sorbed phase contamination in the limestone fractures and matrix. The combined methods were able to provide detailed vertical profiles of DNAPL and contaminant distributions, water flows and fracture zones in the aquifer and are therefore a powerful tool for site investigation. For the limestone aquifer the results indicate horizontal spreading in the upper crushed zone, vertical migration through fractures in the bryozoan limestone down to about 16-18 m depth with some horizontal migration along horizontal fractures within the limestone. Documentation of the DNAPL source in the limestone aquifer was significantly improved by the use of FACT™ and Water FLUTe™ data.

This is a Post Print of the article published online April 6th, 2016 in Journal of Contaminant Hydrology 189 (2016) 68–85. The publishers' version is available at the permanent link: http://dx.doi.org/10.1016/j.jconhyd.2016.03.007

Introduction

Characterization of dense non-aqueous phase liquid (DNAPL) source zone architecture and the dissolved and sorbed contaminant distribution (e.g. secondary source zones) in fractured and dual permeability geologic media is essential for: developing accurate site specific conceptual models; delineating and quantifying contaminant mass; performing risk assessments; and selection and design of remediation alternatives (NAS 2015, Mercer et al. 2010, Kueper and Davies 2009, Feenstra et al. 1998).

Characterization of the contaminant distribution in limestone (or chalk) aquifers is especially challenging due to the heterogeneous nature of the limestone, with highly conductive fractures and variable permeability matrix blocks (Witthüser et al., 2003, Loop and White, 2001, Williams et al., 2006). This requires high-resolution data and unbiased samples of the contaminant distribution (as demonstrated by e.g. Parker et al., 2006, Goode et al., 2014). To date most contaminant investigations and monitoring in limestone/chalk and other fractured rock aquifers have been based on water sampling from traditional open boreholes or screened wells. The methods currently available for characterizing limestone geology and hydrogeology are limited and costly, and high-resolution sampling and analysis is a difficult task. The potential presence of mobile (or residual) DNAPL in unconsolidated materials overlying limestone or within the limestone fractures further complicates drilling/coring in limestone aquifers. For these reasons limestone is an investigative challenge .

Multilevel devices developed for depth-specific groundwater sampling in fractured rock include: the Westbay Multiport System™ (www.westbay.com, Black et al., 1986); the Waterloo system™ (www.solinst.com, Cherry and Johnson, 1982); a modified Waterloo system™ (Parker et al., 2006); the Water FLUTe System™ (www.flut.com, Cherry et al., 2007); and the Continuous Multichannel Tubing (CMT) System™ (www.solinst.com, Einarson and Cherry, 2002). Most of these were designed for deep boreholes (> ~30 m, Einarson, 2006). The Water FLUTe System™ and the modified Waterloo System™ include a large number of sampling intervals (over depth) for high-resolution contamination profiling in relatively shallow boreholes. The modified Waterloo System™ can be used for installations in both unconsolidated and consolidated material because it includes reliable high-resolution seals between intervals which are created by backfilling bentonite and sand around the sampling ports as the outer casing of the rotasonic coring equipment is withdrawn (Parker et al., 2006). The Water FLUTe System™ consists of a blank liner (FLUTe) and a depth discrete multilevel monitoring system (Water FLUTe or FLUTe MLS). The continuous blank liner seals the entire borehole prior to the MLS installation to prevent vertical cross connection, while the MLS is custom designed and allows for borehole logging (Cherry et al., 2007). Transmissivity profiling can be conducted during installation of the blank liner (Keller et al. 2014, Quinn et al. 2015). The MLS seals the entire borehole except for each of the up to 15 individual monitoring intervals. The system can be used to obtain depth discrete monitoring data on hydraulic pressure/head and groundwater quality and includes unique and versatile design features not available by any of the other systems (Cherry et al., 2007).

Several drilling methods are available for limestone. A continuous core and dual casing approach is possible when rotasonic drilling/coring and by wire-line rotary coring (Einarson, 2006). Single casing approaches include ODEX (e.g. Jakobsen et al., 1992) and DTH drilling, but these do not provide continuous cores. Wire-line rotary coring is described in detail in the experimental methods section of this paper. Rotasonic coring with subsequent installation of the Waterloo System™ is described in Parker et al. (2006). A variety of methods are available for core sampling. Sterling et al. (2005) used high-resolution subsampling of cores with an analytical method based on quantitative methanol (water miscible) extraction (Hewitt, 1998) for analysis of chlorinated VOCs

This is a Post Print of the article published online April 6th, 2016 in Journal of Contaminant Hydrology 189 (2016) 68–85. The publishers' version is available at the permanent link: http://dx.doi.org/10.1016/j.jconhyd.2016.03.007

in rock core matrices (dissolved and sorbed), and Lawrence et al. (1990) used water immiscible solvent extractions of chalk core material (crushed in solvent).

Screening tools, such as MIP (membrane interface probing) and LIF (laser induced fluorescence) are available for profiling in unconsolidated materials (Mercer et al., 2010, Fjordbøge et al., 2016). However, they are direct push driven and hence are not applicable in limestone aquifers. In sandy aquifers, partitioning inter-well tracer tests (PITTs) have been used with success to identify and quantify NAPL (Annable, 2008). PITT is dependent on the establishment of a controlled uniform flow field, which is unlikely in fractured limestone aquifers. Similarly, single well push-pull tests with partitioning tracers depend on controlled injection and abstraction that is difficult in fractured limestone. Radon-222 constitutes a naturally occurring partitioning tracer with an affinity for NAPL (Semprini and Istok, 2006, Semprini et al., 2000, Schubert et al., 2007, Ponsin et al., 2015). However, the Radon emanation rates from limestone are low (Gravesen et al. 2010) and background levels in the Naverland limestone were associated with the overlying clay (Janniche et al. 2013).

The FLUTe® techniques are an innovative set of tools for DNAPL documentation and dissolved and sorbed phase contaminant distribution screening and sampling (overview given in Table S1). They include the FLUTe® (flexible liner underground technology) blank liner, NAPL (non-aqueous phase liquid) FLUTe™, Water FLUTe™ (or FLUTe MLS), FLUTe® transmissivity test and FACT™ (FLUTe activated carbon technology) Some of the techniques have been applied at many sites (e.g. NAPL FLUTe™ (Mercer et al., 2010) and Water FLUTe™ (Cherry et al., 2007)), while the FLUTe® transmissivity test (Keller et al., 2014, Quinn et al., 2015) and FACT™ have only recently been developed. The FLUTe® technologies supplement existing sampling methods. The combined use of FACT™, transmissivity and modeling provides an innovative tool in the line of evidence for DNAPL solvent and contaminant distribution in fractured limestone/rock.

The scope of the investigations in the limestone aquifer and focus of this paper is to obtain an improved conceptual understanding of DNAPL source zone architecture and dissolved and sorbed chlorinated compound distribution in bryozoan limestone using a combination of site investigation technologies, including the new FLUTe® transmissivity test and FACT™ techniques. The paper is innovative for limestone aquifers, for which there is a lack of detailed sampling methods for contaminated sites. The field study was supplemented with laboratory experiments and new model-based data interpretation tools to interpret the data obtained with the FACT FLUTe™.

The methods were tested at the Naverland site near Copenhagen, Denmark. The site is a former distribution facility for perchloroethene (PCE) and trichloroethene (TCE) where DNAPL leakage has impacted a fractured clayey till and an underlying fractured limestone aquifer/bedrock. At the site, a wide range of innovative and current site investigative tools for direct and indirect documentation and/or evaluation of DNAPL presence in clayey till (Fjordbøge et al. 2016) and limestone were combined in a multiple lines of evidence approach. Good conceptual understanding of DNAPL transport and distribution in clayey till was obtained, and a set of characterization techniques for investigations of source zone architecture in clayey till was identified by Fjordbøge et al. (2016).

Experimental Methods

The FLUTe® technologies, including NAPL FLUTe™, FACT™, FLUTe® transmissivity profiling, and Water FLUTe™ , were employed in three cored boreholes (C1-C3) in the PCE and TCE DNAPL source zone in the limestone aquifer at the Naverland site. A brief site description and site plan with borehole locations and an overview of FLUTe® technologies are provided in the Supporting Materials (SM, Table S1). The cores from the boreholes were sub-sampled and

This is a Post Print of the article published online April 6th, 2016 in Journal of Contaminant Hydrology 189 (2016) 68–85. The publishers' version is available at the permanent link: http://dx.doi.org/10.1016/j.jconhyd.2016.03.007

analyzed. To improve the understanding of FACT data, the sorption and uptake from contaminants in solution and as DNAPL were tested in the laboratory, and the uptake during installation in a fractured limestone aquifer was modeled.

FACT™ and NAPL membrane Laboratory Testing

To quantify the sorption characteristics of the FACT™, batch experiments were conducted for PCE, TCE, cDCE, and a mixture of these for a range of concentrations and exposure times. The potential effect of the NAPL membrane on the sorption was investigated. A detailed description of the experiments is given in SM. FACT™ DNAPL exposure tests were conducted for water saturated and dry AC to quantify the maximal uptake on AC (see SM). NAPL membrane exposure tests were conducted by exposing a NAPL membrane to TCE and PCE saturated water, as well as DNAPL in the laboratory, and visually inspecting the membrane for transparency as well as staining (or lack of staining) to explore indications of near solubility aqueous concentration as well as DNAPL contact (see SM).

Limestone Aquifer Characteristics

The characteristics of the local geology of the limestone aquifer and overburden were obtained from former site investigations, literature and from contacts at the Geological Survey of Greenland and Denmark (GEUS). A thorough geological characterization of the cores collected in the investigation was conducted after subsampling for VOCs (described below). Depth-dependent data from each core included the geological type and composition, the occurrence of fractures and chert, and the limestone hardness. Subsamples (14) were collected and analyzed by standardized methods (gravimetric) by the Danish Geotechnical Institute to obtain the limestone parameters (porosity, density, water content). Subsamples were collected for biostratigraphic analysis (1 sample from each C2 limestone core, i.e. approximately one sample for every 1.5 m) and analyzed by GEUS. The transition zone was described from samples collected by dry rotary auger drilling prior to the coring of the limestone.

Coring and Subsampling of cores for contaminant analysis

Overburden pre-drilling and limestone coring

Prior to coring the limestone aquifer a PEH casing (OD 225 mm, ID 198 mm) was installed in a 250 mm (10") borehole at each of the three locations C1-C3 by dry rotary auger drilling through the overburden (backfill, clayey till and gravel/crushed limestone) into the top of the limestone at 7.9-8.7 m bgs. This was done to prevent downfall of overburden materials or downward migration of mobile DNAPL from the clayey till sequence in the cored boreholes to the limestone aquifer. The boreholes for the PEH casings were drilled from (inside) pre-installed shallow dry wells (D 600 mm), which subsequently housed the Water FLUTe™ installations.

Cores were collected in PVC liners by wire-line coring by the drilling contractor Aarslev, Denmark. The borehole diameter was 146 mm (~6") and the core diameter was 102 mm (~4"). Wire-line coring was chosen, as it was the only available coring technique used routinely by Danish drilling contractors in limestone aquifers/bedrock. In the wire-line coring technique, a cylindrical sample (core) is cut out of the formation by a rotating drill crown on the outer rotating casing. The core enters the inner wire-line casing (not rotating) with the PVC liner attached to a core-drill-head with a conical core-catcher. For each core collected, the inner (wire-line) casing and core-drill-head is detached from the outer casing and drill-head and brought to the surface. Clean tap water was used as the cooling fluid without recirculation (recovered water was collected and transported to a nearby sewage treatment facility). The cooling water used to cool the drill crown enters between the two casings and returns with cuttings on the outside of the outer casing. Water usage and water-loss

This is a Post Print of the article published online April 6th, 2016 in Journal of Contaminant Hydrology 189 (2016) 68–85. The publishers' version is available at the permanent link: http://dx.doi.org/10.1016/j.jconhyd.2016.03.007

to the formation was minimized. Coring was conducted in (up to) 1.5 m long sections. However, for some sections significant core loss occurred. After each cored section was retrieved, the bottom of the borehole was checked for DNAPL (down-hole dual phase sensor (Solinst interphase meter®) and/or liquid sampling) with instructions to stop drilling, if there were any signs of significant DNAPL mobilization in the borehole. No measurable DNAPL was encountered. The PVC liners were cut to an appropriate length on site and capped, then transported in angled position with the bottom down to the laboratory where they were stored outdoors at ~5-10˚C until subsampled. Subsampling was conducted as soon as possible and within a few days of collection (the laboratory sampling crew was unable to keep up with the coring). When the required depth for the coring (20 m bgs.) was reached, the outer casing was retracted and the open borehole was purged to remove cooling water lost to the formation. The pump was placed at the depths where most water was lost to the formation during coring. The borehole was left open for the shortest possible period before a FLUTe® liner with NAPL cover and FACT™ was installed.

Screening and subsampling of cores, and extraction for quantitative analysis

In the laboratory, the core liner was split open and the core covered with Rilsan® foil in a vented hood. PID screening (photo-ionization detector, Microtip, 10.6 eV Krypton PID lamp) was conducted immediately under the foil and prominent geologic information was mapped by observation through the foil, such as fractures, color, and chert content. The PID screening (data not shown) was used to select sampling locations and discretization. The greatest discretization was selected for sections with a relatively high PID response so as not to miss small high concentration locations. In addition, subsamples of limestone collected during the subsequent sampling were placed in air filled Rilsan bags and left at room temperature (~20˚C) overnight for equilibration and subsequent PID measurement.

Subsamples of ~5 g were collected from the cores with stainless steel tools (beneath the core surfaces) and immediately transferred to 20 mL glass vials with screw-caps with teflon lined septa containing 10 mL tap-water, then 5 mL pentane with internal standard was added. To minimize the potential effect of volatile loss from exposed surfaces during transport and storage in sealed PVC liners, and during subsampling, a few mm (3-5 if possible) of the exposed surface was discarded before the subsample was taken/transferred to the vial. With the low diffusion rate in saturated limestone, this was expected to suffice. The samples were hand-shaken and vortexed to disperse the limestone in the water and then placed in a rotation box at 10˚C overnight to complete the extraction of contaminants. The extraction technique for the limestone samples was adapted from a technique developed and previously used for solvents in clay till samples by Scheutz et al. (2010), Damgaard et al. (2013a+b), and Fjordbøge et al. (2016). It exploits a combination of the water and matrix porewater miscibility and the efficiency of immiscible solvent (pentane) extraction – combining and refining the methods of Sterling et al. (2005) and Lawrence et al. (1990), respectively. Three subsamples of each extract were transferred to GC-MS vials. One subsample was analyzed for PCE, TCE, cDCE and TCA (limestone analysis, see below), and the others stored as back-ups and for potential dilution.

A subsample from a high PID response zone was tested for NAPL using the SudanIV test kit (OilScreenSoil™ (SudanIV) from Cheiron Resources Ltd) as prescribed by vendor. No response for NAPL was observed (data not shown). As the PID measurements never exceeded the level at which NAPL test kits have previously been observed to give a positive response (Fjordbøge et al., 2016), Sudan(IV) tests were not performed for any other samples from the limestone cores.

NAPL FLUTe and FACT Installation and Subsampling

This is a Post Print of the article published online April 6th, 2016 in Journal of Contaminant Hydrology 189 (2016) 68–85. The publishers' version is available at the permanent link: http://dx.doi.org/10.1016/j.jconhyd.2016.03.007

A FACT™ was installed in each limestone borehole immediately after the borehole had been purged, with two strips on opposite sides of a NAPL FLUTe™. A down-hole dual phase censor (Solinst Interface Meter®) was used to detect if DNAPL was present in the bottom of the boreholes every time the boreholes were open. The FACT™ dimensions used in this study are shown in Table 1. The inverted liner was everted towards the borehole wall in a few seconds, thereby minimizing the exposure to borehole water. The AC strips were protected by an aluminum foil on one side and a NAPL cover on the other. The NAPL cover was highly hydrophobic and only permeable to water through small perforations (horizontal). As the FACT™ is installed water is forced out of the borehole – preferentially into high conductivity fractures/zones. In zones with lower conductivity, borehole water can be forced down the hole to higher conductivity fractures/zones potentially affecting AC concentration. The FACTs™ were retracted after 42 hours of exposure and initial sample processing was done on-site. The exposure time was selected based on: a) preliminary sorption tests (Beyer, 2012) which showed that more than 95% of equilibrium sorption was reached within 42 hours (later experimental investigations reported in the SM of this paper revealed longer timeframes), b) concerns of saturation of sorption sites in thin AC, and c) to manage cost (on-site technical staff availability). However, given disturbances due to drilling and pumping activities and installation a long exposure time can be advantageous. The NAPL FLUTe™ was cut open and screened along its entire length with a PID and inspected for smeared hydrophobic dye stains to identify zones with high concentrations, where very high-resolution sampling was performed. No DNAPL stains were observed, but some zones showed indications of exposure to solvent saturated aqueous phase (transparency of the NAPL membrane). One of the AC strips was cut in two (vertically). One half was sampled by cutting it into 2-10 cm long subsamples depending on sampling resolution. AC samples were immediately transferred to 20 mL glass vials with screw-caps and Teflon coated septa containing 10 mL tap-water and placed upside down in a cooler with freeze-packs for transportation. The other half was cut into 30 cm lengths, wrapped in aluminum foil and placed in Rilsan® bags in a cooler.

At the laboratory, 3 mL pentane with an internal standard was added to each vial. These were placed in a rotating box at 10˚C for 3-4 days for extraction. Two subsamples of the extracts were transferred to GC-MS vials. One subsample was analyzed for PCE, TCE, cDCE and TCA (AC analysis, see below), the other was kept as a back-up and for potential dilution. Selected 30 cm length of AC were transferred to larger vials containing 30 mL water and 9 mL pentane with an internal standard added and an extraction completed as described above.

High extraction efficiency was documented by setting up batches with a PCE, TCE or cDCE solution in water with and without a submerged piece of AC, letting them equilibrate for 24 hours, and then extracting the entire batch. Controls were set up with pure water and a PCE, TCE or cDCE solution in pentane added at the same concentration as expected in pentane extracts of other batches at the completion of extraction. Concentration differences between vials with and without AC were <10% at equilibrium.

FLUTe Transmissivity Profiling

FLUTe® transmissivity profiling (described in detail by Keller et al. 2014 and Quin et al. 2015) was conducted in each of the three boreholes immediately after retracting the FACT™ NAPL FLUTe™ from the hole.

A blank liner (FLUTe®) was used for transmissivity profiling and to seal the borehole. The FLUTe® blank liner dimensions used in this study are shown in Table 1. To facilitate a complete seal against the borehole wall the liner was oversized. This ensured a good seal even in zones, where the borehole wall was uneven or widens (due to wall collapse). The liner velocity and the water pressure of the liner were measured as it descended during the hydraulic profiling, illustrated

This is a Post Print of the article published online April 6th, 2016 in Journal of Contaminant Hydrology 189 (2016) 68–85. The publishers' version is available at the permanent link: http://dx.doi.org/10.1016/j.jconhyd.2016.03.007

in SM Figure S2. The flowrate is the liner velocity multiplied by the borehole cross section. The flowrate per unit delivery/driving pressure was plotted against depth and transformed to a transmissivity for each time-step and depth using Darcys law, and then averaged over specific depth intervals (0.32 m). The transmissivity was then transformed to a hydraulic conductivity for each depth interval (as described by Keller et al. 2014). The liner velocity is affected in zones where the borehole widens e.g. due to borehole wall collapse. For these zones, the transmissivity inferred for the section by the change between the entrance and the exit of the enlargement was assigned to the entrance of the enlargement. The total borehole transmissivity was preserved. The blank liners were left in the borehole as a seal while Water FLUTes™ were designed and prepared.

Water FLUTe™ Design, Installation and Sampling

A Water FLUTe™ (described in detail by Cherry et al., 2007) was designed for groundwater sampling of each borehole using information on the concentration profile obtained from core and FACT™ subsampling and analysis, and the transmissivity profile for each borehole. The design was sent to FLUTe®, who manufactured the Water FLUTes™. Each FLUTe™ had 12-13 sampling intervals/ports with the sampling intervals set by an external spacer on the liner and a dedicated pumping system on the interior of the liner. A positive gas displacement system was employed to drive the sample water to the surface. The sampling intervals/ports were separated by minimum 30 cm to ensure hydraulic separation of sampling intervals. Water FLUTe™ dimensions used in this study are shown in Table 1. The blank liners were retracted and the Water FLUTes™ immediately installed in the boreholes (to minimize open borehole time) a few months after the boreholes had been cored. The preparation and installation procedure for Water FLUTe™ was described by Cherry et al. (2007). More details on the shipment, preparation and installation process of the C1-C3 Water FLUTes™ at Naverland is provided in the SM.

The system was tested after the wellhead installation process was completed. As part of the test procedure, each port was purged two times while monitoring purge volumes and recharge rates. Purging each port took less than 15 min. At the end of testing a water level meter was used to measure water levels in each tube. At C1 the targeted borehole depth was shorter (by 0.6 m) than the Water FLUTe™. Therefore, sampling interval (spacer) #12 (17.00 m – 17.40 m) was only partially everted by 0.09 m (i.e. only 0.09 m of the 0.4 m long sampling interval is in contact with the borehole wall) which is just enough for the spacer to function properly. Unfortunately, C2 had a very slow leak (not detectable while installing). The liner may be filled with a bentonite slurry at 60 mPa·s to stop the very slow leak as recommended by the manufacturer.

The Water FLUTes™ were sampled shortly after the installation (Sampling event 1) and again ~3 weeks later (Sampling event 2) after discontinuance of remedial pumping at the site (described below). The sampling ports were entirely purged and sampled simultaneously using a six port sampling manifold designed by FLUTe® and analytical grade nitrogen gas following the sampling guidelines by FLUTe®. Each sampling port was purged 4 times (when possible) prior to sampling. The purge volume was equivalent to the water volume in the tubing and spacer (~4 L for a 30 cm port). The pressure was lowered to a sampling pressure (lower flow than for purging) and a volume discarded before the actual sample was taken. Water samples were placed upside down in coolers with freezer packs and transported to the laboratory for analysis, see analytical methods below.

Concentration Rebound Test

It was hypothesized that remedial pumping at the site (in K11) could be causing dilution of the contaminant by water inflow through fractures/conductive parts of the limestone. To examine the impact of remedial pumping, a concentration rebound test was conducted. The remedial

This is a Post Print of the article published online April 6th, 2016 in Journal of Contaminant Hydrology 189 (2016) 68–85. The publishers' version is available at the permanent link: http://dx.doi.org/10.1016/j.jconhyd.2016.03.007

pumping was turned off (2 days after sampling event 1) and the hydraulic head/pressure changes in the Water FLUTe^{TM} multilevel ports monitored until a stable pressure profile was observed (SM Figure S4). Approximately 3 weeks after termination of remedial pumping, a new set of water samples was collected and analyzed (Sampling event 2).

Analytical Methods

GC-MS (Gas Chromatography with Mass Spectrometry detection). The analytes (PCE, TCE, cDCE, TCA) were separated and identified by GC-MS using an Agilent 7980 gas chromatograph system equipped with a Agilent 5975C electron impact (70 eV) triple-axis mass-selective detector. The mass-selective detector temperature was 230°C for the electron impact source and 150°C for the quadrupole with the transfer line held at 250°Cand the spectra were measured in selected ion monitoring. Chloroform was used as internal standard and detection and quantification limits were determined as described by Winslow et al. (2006). Concentration levels of TCA and cDCE were negligible compared to PCE and TCE levels and so are not described here.

Limestone and AC extracts. A 0.5 µL pentane extract was injected at 250°C with a 5:1 split ratio. Chromatographic separation was achieved on a 30 m x 0.25 mm I.D. x 1.40 µm film thickness ZB-624 capillary column (Phenomenex). The initial column temperature was held at 40°C for 3 min. then increased at 20°C min^{-1} to 150°C for 2 min., and 50°C min^{-1} to 260°C for 1 min. The total run time was 13.7 min. with Helium (1.1 mL min^{-1}) as carrier gas.

Water samples. 4 mL samples were injected into sealed vials, acidified with 0.5 mL 4% H_2SO_4 and incubated in a rotary shaker at 250 rpm and 85°C for 5 min. A 2 mL headspace was injected in splitless mode at 80°C. Chromatographic separation was achieved on a 30 m x 0.32 mm I.D x 20.00 µm film thickness HP-PLOT/Q capillary column (Agilent Technologies). The initial column temperature was set to 40°C for 4 min. then increased with 35°C min^{-1} to 290°C. The final temperature was held for 7 min and the total run time was 18.1 min. with Helium (1.6 mL min^{-1}) as carrier gas.

Data Treatment

Phase partitioning calculations were conducted using the PCE and TCE concentrations in the limestone samples to determine phase composition and effective solubility for each compound, as described for clayey till samples in Fjordbøge et al. (2016). For calculations, the average porosity (C1: 0.4) and bulk density (C1: 1.75 g/cm^3) measured for each cored borehole, solubility reported by Broholm and Feenstra (1995, PCE: 240 mg/L, TCE: 1400 mg/L), and K_d values estimated by use of the Piwoni and Banerjee (1989) equation (PCE: 0.28 L/Kg; TCE: 0.12 L/Kg) were applied. Calculations were also performed with sorption coefficients for Danish limestone from the Copenhagen area (not Naverland, but of similar origin and with similar characteristics such as organic carbon content) determined by Salzer (2013) for PCE (0.49-1.13 L/Kg) and TCE (0.19-0.42 L/Kg). If the calculations indicated that DNAPL was present in the core subsamples, then the DNAPL saturation was calculated.

Likewise, the measured groundwater concentrations were compared with the calculated effective solubilities to evaluate whether DNAPL was likely to be present.

FACT^{TM} concentrations were transformed to porewater concentrations using the model and parameters described below, and then compared to measured limestone and groundwater concentrations.

FACT^{TM} Exposure Model

The sorbed contaminant concentrations measured on the FACT^{TM} are influenced by the flow and transport processes around the borehole; hence, they cannot be directly related to aqueous

This is a Post Print of the article published online April 6th, 2016 in Journal of Contaminant Hydrology 189 (2016) 68–85. The publishers' version is available at the permanent link: http://dx.doi.org/10.1016/j.jconhyd.2016.03.007

porewater concentrations. To aid with the understanding and interpretation of the measured concentrations on the activated carbon strips (FACT™), a COMSOL Multiphysics® model was constructed. The model simulated the accumulation of the contaminant in the FACT™ during its exposure time and the flow and transport in the limestone aquifer surrounding the borehole.

Single-phase flow with contaminant transport was simulated within the entire domain. The stationary flow was described using the groundwater flow equation:

$$\nabla \cdot \mathbf{q} = \nabla \cdot (-\mathbf{K}\nabla H) = 0,$$

with the water flux **q** approximated by Darcys law, the hydraulic conductivity **K,** and the hydraulic head H.

The governing equation for dissolved contaminant transport including advective transport, diffusive transport and sorption:

$$\left(1 + \frac{\rho_b k_d}{n}\right)\frac{\delta c}{\delta t} + \nabla \cdot (\mathbf{q}c) - \nabla \cdot (\mathbf{D}\nabla c) = 0,$$

with the bulk density ρ_b, sorption coefficient k_d (linear sorption is assumed), porosity n, contaminant concentration c, and the dispersion tensor **D**.

The equations were solved for a 2-D cross section through the borehole (top view) including the installed FACT™ and the surrounding aquifer with groundwater flow. A grid convergence study guided with the required grid resolution. With a compressed thickness of ~0.5 mm, the transport and sorption processes in the FACT™ require a resolution by very fine elements and the resultant finite element mesh consists of 0.5 – 2 million elements. When appropriate, the symmetry of the domain was exploited to reduce computational efforts. An overview of the model domain and boundary conditions are shown in Figure 1 and the parameters in Table 2.

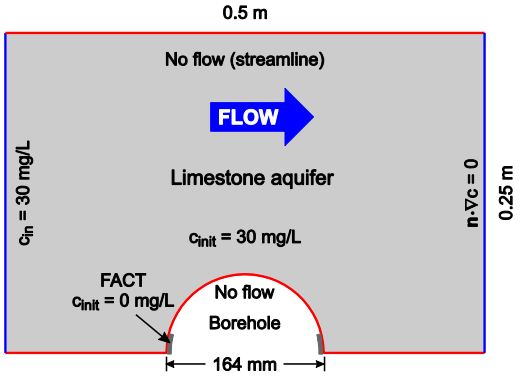

Figure 1: Model set-up for FACT contaminant uptake.

Results and Discussion

Limestone Core Recovery

Wireline coring was recommended in limestone by Danish drilling companies based on their experience from the Copenhagen Metro City-Ring and Copenhagen-Ringsted railway-line investigations. The uppermost, often brecciated limestone, is typically screened off before coring commences to avoid loose material falling into the borehole. This procedure was also followed

This is a Post Print of the article published online April 6th, 2016 in Journal of Contaminant Hydrology 189 (2016) 68–85. The publishers' version is available at the permanent link: http://dx.doi.org/10.1016/j.jconhyd.2016.03.007

here, mainly to limit the risk of DNAPL migration down the borehole. However, some fall-in of material in the borehole C1 did occur in the uppermost zone where a sub-vertical fracture was observed in the core, with resultant accumulation of sediment at the bottom of the hole. The core recovery and geologic features observed during core subsampling are shown for each of the three boreholes in Figure 2.

Significant core loss occurred at some depths, most often where the recovered core consisted of chert/chert nodules. There, the loss was thought to have been caused when soft limestone adjacent to chert (or harder/more cemented limestone) was flushed out when drilling through the chert/hard limestone where more cooling water was required for the drill bits. The loss of softer more permeable zones during coring strongly suggests that chlorinated ethenes including DNAPL was lost adjacent to/in these zones in the cores. Relatively few core subsamples could be collected from these cores/zones (chert was not sampled). This is a significant limitation of the wireline coring method for characterization of DNAPL architecture in limestone aquifers/bedrock.

The core loss is also likely to have affected the comparison of geology/fracturing with hydraulic profiling, and the comparison of contaminant concentrations in limestone samples with concentrations in water and FACT^{TM} samples.

Site Limestone Geology

The limestone aquifer at Naverland is overlain by two clay till units deposited during the two most recent glacial events (described in Fjordbøge et al. 2016). A transition zone of mixed glacial sand/gravel/clay and brecciated (crushed up) limestone, also known as glacitectonite (Pedersen, 2014 and 1988), is located between the intact limestone and the clay till. At Naverland, the transition zone is 0.7-1.1 m thick and consists of gravel, sand and brecciated limestone with chert. The actual limestone aquifer is a Stevns formation bryozoan limestone (Danien period in Paleogene time), mainly consisting of calcite (>90% $CaCO_3$) with interbedded chert layers and nodules (e.g. Brotzen et al. 1959, Stenestad 1976). Based on the biostratigraphic analysis, the sampled section was deposited in the middle Danien period and includes the bottom of the upper bryozoan mound complex to top of the middle bryozoan mound complex. All five samples collected from each 1.5 m cored section between 9 and 18 m bgs. represent biostratigraphic unit NNP2F (Varol et al., 1998) according to GEO and GEUS (2014).

The limestone aquifer is fractured. Horizontal fractures and chert layers are likely to have the same bryozoan mound structure observed at the nearby Stevns Klint, Karlstrup quarry (lower bryozoan bank, Damholt and Surlyk 2014, and Surlyk et al. 2006) and Limhamn quarry (upper and middle bryozoan banks, Brotzen 1959). The lower mounds at Stevns and Karlstrup are 50-300 m long and 45-110 m wide, while the middle and upper mounds have a smaller and variable length to width ratio (GEO and GEUS 2014). Based on the evidence from the quarries, the horizontal fractures are thought to be closely spaced at the top of the limestone and then decrease in density with depth. The middle and upper bryozoan mounds are thought to be separated by a horizontal hard ground approximately located in the upper 5 m of the limestone (GEO and GEUS, 2014). The hardground is not expected to follow the mound structure. Multiple fractures were observed in the limestone cores of boreholes C1-C3. However, the majority of these are likely to have been caused by the drilling. Hence, it was not possible to estimate the horizontal fracture spacing. Based on observations at Karlstrup (Madsen, 2003) fractures are associated with limestone-chert layer interfaces and so are expected to have a spacing of 0.1-1 m. Due to the mound structure of bryozoan limestone, it is not surprising that there was little horizontal correlation of the layers between the boreholes. The exception being the horizontal chert layer in the upper part of the limestone which may be associated with the hardground separating the upper and middle bryozoan banks. Dipping vertical fractures (which appeared natural) were observed in some cores from the boreholes.

This is a Post Print of the article published online April 6th, 2016 in Journal of Contaminant Hydrology 189 (2016) 68–85. The publishers' version is available at the permanent link: http://dx.doi.org/10.1016/j.jconhyd.2016.03.007

Vertical fractures were expected to occur at depths of up to 35-50 m bgs, with the highest density in the upper 10-15 m of the limestone and an approximate spacing of 3-4 m (GEO and GEUS, 2014). Based on the direction of known faults in the limestone in the region, the dominant directions of the vertical fractures were expected to be NNW-SSE and WSW-ENE (GEO and GEUS, 2014). The limestone is underlain by white cretaceous chalk at 40-50 m bgs at the site (Geoviden 2014 referencing Lyell 1837).

The porosity of the limestone at C1, C2 and C3 ranged from 13% to 48% with an average 33%, with the majority (9 of 14) being within a range of 29-40%. The bulk density ranged between 1.42 and 2.36 g/cm^3 and was inversely correlated with the porosity. Soft limestone had a large porosity (>38%), while the lowest porosity was found for hard limestone (from 13%). However, relatively large porosities (up to 40%) were also observed for hard limestone and limestone of intermediate hardness. Samples of hard limestone retrieved during drilling (not cored) at other locations at the site had porosities ranging between 14-19%. The range of horizontal matrix hydraulic conductivities of these hard limestone samples (determined by standard poro-perm tests at GEO) was 1.7-6.4·10^{-9} m/s and slightly lower vertically (1 sample).

The hydraulic conductivity and porosity measurements compared well with other limestone datasets (GEO and GEUS, 2014). Based on this, the matrix hydraulic conductivities for the high porosity samples (including the soft samples) were expected to be in the 10^{-7}-10^{-6} m/s range (2 orders of magnitude higher than for the hard low porosity samples). Madsen (2003) observed a strong relationship between porosity and matrix permeability in vertical profiles at Karlstrup quarry with porosities ranging between 20-50% and hydraulic conductivities between 10^{-7} and 10^{-6} m/s. The highest porosities and conductivities were shown to occur in softer limestone close to chert layers in the bryozoan mounds. GEO and GEUS (2014) suggested that SiO_2 dissolution occurred (from shells) during the formation (growth) of the chert layers, with zones of high flows in the limestone being associated with soft limestone and fractures adjacent to the chert layers and nodules. Their results suggest that core loss occurs in the soft limestone adjacent to chert layers, resulting in the dominance of chert in the collected cores.

The observations in the cores collected from C1-C3 (Figure 2) lead to the following geologic conclusions:

- Larger chert layers occur in the upper part of the limestone (down to 10-11 m bgs., or 2-4 m below the top of the limestone). These may be associated with the hardground separating the upper and middle bryozoan banks. The chert layers are typically 10-30 cm thick. The bottom of the deepest chert layer (~20 cm thick) in the three boreholes appears to dip about 5-10˚ in the north to northwesterly direction. However, due to core loss and fracturing induced by the drilling this conclusion is somewhat uncertain.
- Layers with chert nodules were observed between 12 and 16 m bgs. at C1 and C2 and around 19 m bgs. at C1.
- The hardness of the limestone increased with depth/towards the bottom of the boreholes, particularly at C3.
- There are several zones with softer limestone in all three boreholes. These are typically associated with sections with significant core loss.
- Fractures were less common in the harder zones of the limestone. Fractures are predominantly found in the softer limestone, often close to chert layers or internally in thicker zones of harder limestone.

This is a Post Print of the article published online April 6th, 2016 in Journal of Contaminant Hydrology 189 (2016) 68–85. The publishers' version is available at the permanent link: http://dx.doi.org/10.1016/j.jconhyd.2016.03.007

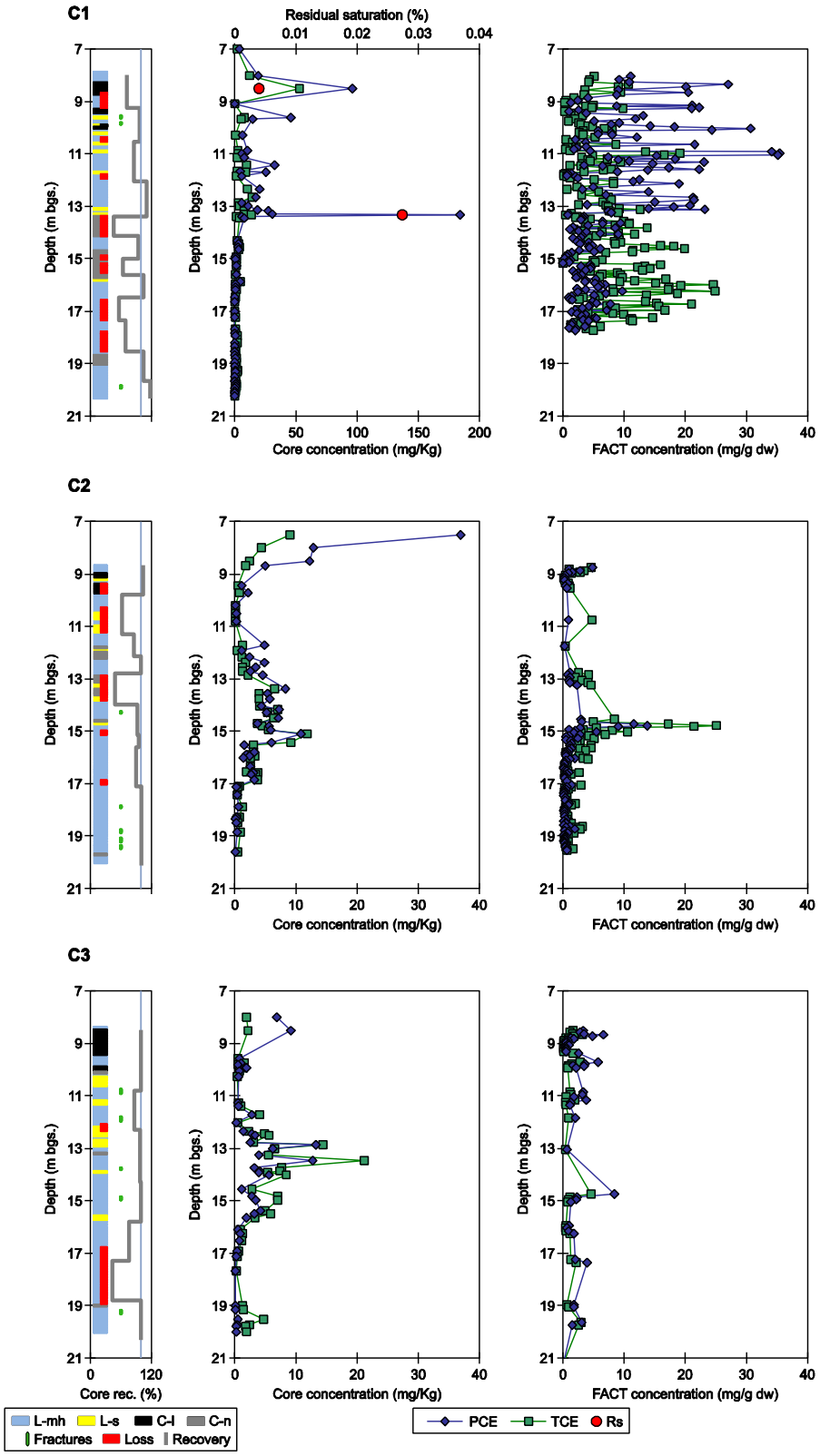

Figure 2. Limestone core descriptions, core recovery, core concentrations, DNAPL residual saturation (Rs) and FACT^{TM} concentrations for boreholes C1-C3. Note that the core concentration axis for C1 differs from C2 and C3, whereas the FACT^{TM} concentration axis are the same for all

This is a Post Print of the article published online April 6th, 2016 in Journal of Contaminant Hydrology 189 (2016) 68–85. The publishers' version is available at the permanent link: http://dx.doi.org/10.1016/j.jconhyd.2016.03.007

three. L-mh: Limestone medium to hard, L-s: Limestone soft, C-l: Chert layer, C-n: Chert nodules, dw: dry weight.

Chlorinated Solvent Content in Limestone Samples

The concentrations of PCE and TCE in limestone samples are shown as depth profiles for each of the boreholes in Figure 2. DNAPL was documented (SudanIV tests) in the transition zone (gravel, brecciated limestone) in a borehole cored through the clayey till just southwest of limestone borehole C1 (Fjordbøge et al. 2016, SM Figure S1 cored borehole CT2). Boreholes C1, C3 and CT2 are located in an area with a relatively thin zone of reduced clayey till overlying the limestone, with dipping vertical fractures penetrating the clayey till unit (Fjordbøge et al., 2016).

For C1 a relatively high PID response (data not shown) of 650-1500 ppm (as isobutylene gas) was observed in the upper limestone (7-8.5 m bgs.) above the upper chert layer (~8.3-8.8 m bgs.). Below this and down to a chert nodule layer (~13.4-13.8 m bgs.) PID responses generally ranged between 50 and 300 ppm, with one exception at 13.32 m bgs. where a PID response of 1370 ppm was recorded. At > 14 m bgs. most PID responses were lower than 50 ppm with a few being up to 100 ppm.

The concentration of PCE in C1 was quite variable, with levels between about 6 mg/kg and 50 mg/kg for most limestone samples down to 14.4 m bgs., with 2 exceptionally high PCE concentrations of 184 mg/kg at 13.32 m bgs. and 98 mg/kg at 8.5 m bgs. TCE concentrations were generally lower and followed practically the same (though not identical) pattern. At greater depth (>14 m bgs.) both PCE and TCE concentrations were generally lower than 3 mg/kg with one exception at 15.86 m bgs., where both were about 4.5 mg/kg. At these deeper depths, TCE tended to dominate over PCE.

The two highest PCE concentrations (184 mg/kg at 13.32 m bgs. and 98 mg/kg at 8.5 m bgs) seen at C1 reach levels indicating the presence of DNAPL. For these samples a residual saturation of approximately 0.027% and 0.004%, respectively was calculated using the K_d estimated by the Piwoni and Banerjee (1989) equation. If the lowest limestone K_d determined in experiments on limestone core material (Salzer, 2013) is used, only one sample is found to contain DNAPL, at a residual saturation of 0.015%. With the highest K_d from Salzer (2013) none of the samples are found to contain DNAPL. The calculations of residual saturation assume an even distribution of contaminant in the pore space of the sample. However, DNAPL is likely to be found in fractures which are only a minor part of the total porosity. Hence, the residual saturation in a fracture may be significantly higher (e.g. 100 times if 100 µm fracture in 1 cc sample). The two C1 samples with highest concentration were collected just above layers with chert nodules. A SudanIV test at the upper depth did not indicate NAPL. However, this is not surprising given that Fjordbøge et al. (2016) reported a detection limit of 250 mg/kg for SudanIV tests on clayey till samples, and uncertain color observations up to 1500 mg/kg for PCE.

For cores from boreholes C2 and C3, all PID responses were <50 ppm except at a few locations at or above 8 m bgs., where concentrations up to 100 ppm were recorded. The highest PCE concentration at C2 (39 mg/kg) was recorded in the uppermost limestone sample (7.5 m bgs.), a level insufficient to indicate NAPL. For all other depths at C2 and C3 the concentrations of PCE and TCE were <15 mg/kg. PCE and TCE concentrations were only more than 6 mg/kg at 7.5-8.5 m bgs. and 13.37-15.43 m bgs. at C2, and 8.0-8.5 m bgs. and 12.86-14.02 m bgs in C3. The top of these intervals in both C2 and C3 were just above the upper chert layer. At C2 the bottom of the intervals was just beneath a zone with chert nodules and significant core loss. At C3 the depths with high concentrations occurred in a zone of softer limestone.

This is a Post Print of the article published online April 6th, 2016 in Journal of Contaminant Hydrology 189 (2016) 68–85. The publishers' version is available at the permanent link: http://dx.doi.org/10.1016/j.jconhyd.2016.03.007

Chlorinated Solvent Contents on FACT™

Sorption on AC

The time to equilibrium results for PCE sorption on AC from aqueous solution are shown in SM Figure S5, and linear sorption isotherms for PCE, TCE and cDCE for single compounds and for a mixture of the three compounds in aqueous solution are shown in Figure S6a-c. More than 50% of the sorption occurs within 24 hours (~60% in 42 hours) but equilibrium was only reached after 6-7 days at the high solution to AC ratio necessary. Chlorinated ethenes are very strongly sorbed on AC and K_d values for the individual compounds were 12000 L/kg for PCE, 10000 L/kg for TCE, and 3000 L/kg for cDCE. When a mixture of PCE, TCE and cDCE was tested (with equal initial concentrations), a clear competitive effect of PCE on TCE and cDCE sorption was observed at high PCE concentrations (>~0.5 mg/L). This is consistent with findings by Erto et al. (2011), Clausse et al. (1998) and O'Connor (2001) for competitive sorption on granular activated carbon. Further details are provided in the SM.

In the short (42 hour) field deployment/exposure of the FACT™, PCE only migrated a very short distance into the AC strip. Therefore competitive sorption is not likely to have had any effect on the total TCE or cDCE uptake on the FACT™.

Results of the AC DNAPL exposure test suggest a maximum sorption capacity for AC of around 600 mg/g dw AC (the calculated sorbed concentration with a K_d of 12000 L/kg for an aqueous concentration at saturation is 2.88 g/g dw AC). Details are provided in the SM. In the absence of water, a 10 times higher concentration (~6 g/g dw) was found on the AC, probably because of DNAPL trapping in the AC-felt pores.

FACT™ chlorinated solvent concentrations after field exposure

The concentrations of PCE and TCE on the AC samples after 42 hours exposure in the boreholes C1-C3 are shown in Figure 2.

In general, concentrations vary greatly with depth, illustrating the importance of discrete sampling for determining the contaminant distribution and contaminant/source mass in the subsurface. The FACT™ provides possibility for depth specific sampling with a very detailed discretization (cm-scale) over the entire depth of the borehole. This contrasts with techniques such as core sampling, which was particularly challenging at depths with varying limestone hardness, such as where chert layers or nodules were present or for softer intervals, which lead to incomplete core recovery. The high variation in discrete sample concentrations indicates a good seal was obtained against the borehole wall during FACT™ exposure, and that water mixing between the wall and liner had been avoided, even in zones where the borehole was widened (wall collapse).

For borehole C1, PCE dominated in the upper section 8.0-13.3 m bgs., PCE and TCE were present in equal concentrations between 13.3 and 14.2 m bgs., and TCE dominated in the deeper section 14.2-17.7 m bgs. Within each of the three depth intervals PCE and TCE appeared to be strongly correlated suggesting that each zone had a distinct and relatively homogeneous contaminant composition. On a molar basis, PCE dominates to ~13.0 m bgs. and TCE dominates from ~13.5 m bgs. The change in composition on the FACT as well as in core subsamples suggests that little movement of water and contaminants down the hole occurred during installation.

Very large variations in concentrations of PCE and TCE were observed over short distances throughout the cored borehole. In some cases the change in concentration was very abrupt (e.g. at 10.9 m bgs. an increase in PCE from 4.4 to 34.1 mg/g dry weight (dw) is observed within 5 cm), but often the contaminant distribution had an appearance as a diffusion profile (e.g 10.03 m bgs. peak in PCE of 30.7 mg/g dw decrease gradually towards 9.75 m bgs. to 5.1 mg/g dw). The sudden/abrupt increase in concentration on the FACT™ may have been caused by flow-controlled

This is a Post Print of the article published online April 6th, 2016 in Journal of Contaminant Hydrology 189 (2016) 68–85. The publishers' version is available at the permanent link: http://dx.doi.org/10.1016/j.jconhyd.2016.03.007

uptake in a fracture/permeable feature. PCE concentrations in AC samples from the upper section (8.0-13.3 m bgs.) varied between ~1 and 35.4 mg/g dw, with a large number of samples exceeding 10 mg/g dw (39 of 77 samples). Several had peak concentrations around 20 mg/g dw (~12), and a few (3) had peak concentrations exceeding 25 mg/g dw: 27.0 mg/g dw at 8.4 m bgs., 30.7 mg/g dw at 10.0 m bgs. and 34.1-35.4 mg/g dw (3 samples) at 10.9-11.0 m bgs. At greater depth (13.3-17.7 m bgs.) the PCE concentrations were lower than 10 mg/g dw, and most fell within the 2-5 mg/g dw range. Almost half of the TCE concentrations in the deeper section fell in the 10-25 mg/g dw range (29 of 66), the other half and most concentrations in the upper and middle sections were lower than 10 mg/g dw.

The laboratory batch experiments showed an equilibrium PCE concentration of 600 mg/g dw on AC at aqueous PCE saturation. Even if PCE DNAPL was present in the vicinity of the borehole, a concentration of this magnitude was not expected within the exposure time due to limitations on uptake on the FACT^{TM} by diffusion through the limestone matrix. Hence, it is not surprising that the highest concentrations were only 4.5-6% of saturation and most peak concentrations ~3.3%. The highest PCE concentrations on the FACT^{TM} of about 20-25 mg/g dw were observed in the vicinity of the 2 concentration maxima of the limestone core samples. These results suggest that AC PCE concentrations of greater than 20 mg/g dw may indicate presence of DNAPL in/at the borehole. This result is particular for the local contaminant composition and AC exposure time used at the site. Results correspond well with observations by Fjordbøge et al. (2016) of NAPL FLUTe^{TM} staining being observed with AC PCE concentrations above 20 mg/g dw (and always for AC PCE >115 mg/g dw, 24 h exposure time) in clay till. At C1 18 AC samples (~12 peaks) had PCE concentrations >20 mg/g dw, all within the upper section (8.0-13.3 m bgs.). For the water saturated limestone, where uptake over time is limited compared to available capacity of the thin AC strip, a longer deployment/exposure time can be recommended.

The depth distribution observed with the FACT^{TM} compares well with the overall trend of PCE concentrations in limestone core samples if the two maximum limestone sample concentrations and 5 maximum AC sample concentrations are ignored. The lowest levels of PCE in the limestone cores and on the FACT^{TM} were around 5 mg/kg and 3 mg/g dw respectively, and high levels were 15-35 mg/kg and 10-25 mg/g dw respectively. Discrepancies between the FACT^{TM} and core sampling are discussed further in a subsequent section.

For both limestone and AC samples PCE dominates in the upper section, and TCE dominates in the deeper section. However, it appears as if the magnitude of TCE concentrations on the FACT^{TM} in the deeper section is much greater relative to concentrations in limestone when compared to the PCE and TCE ratio in the upper part. This may be explained by the higher effective diffusion rate (lower sorption coefficient and higher free aqueous diffusion coefficient) of TCE in limestone compared to PCE. Competitive sorption would have the same effect, but is not expected for the short deployment time.

For C2 and C3, AC PCE and TCE concentrations were lower than 10 mg/g dw with few exceptions. For C3, PCE generally dominates, whereas for C2, TCE dominates (this would not be the case if normalized by compound solubility). Maximum PCE concentrations at C2 were 11.5-13.8 mg/g dw at 14.7-14.8 m bgs. and 4.6 mg/g dw at 8.8 m bgs.; and at C3 8.4 mg/g dw at 14.4 m bgs. and 6.6 mg/g dw at 8.7 m bgs. Maximum TCE at C2 were 10.6-25.1 mg/g dw at 14.7-15.0 m bgs. and 4.5 mg/g dw at 8.8 m bgs. At C2 there is a quite good correlation with limestone core sample concentrations, whereas at C3 the correlation is not so convincing (possibly because few AC samples were collected in the zone 13-15 m bgs.).

The extensive vertical section with very high PCE concentrations at C1 shows that the borehole was placed in the source area and that there has been a significant downward migration of DNAPL. The more discrete occurrences of high PCE concentrations at C2 and C3 indicate lateral

This is a Post Print of the article published online April 6th, 2016 in Journal of Contaminant Hydrology 189 (2016) 68–85. The publishers' version is available at the permanent link: http://dx.doi.org/10.1016/j.jconhyd.2016.03.007

migration of DNAPL has occurred to these locations, possibly through horizontal fractures. Sub-vertical fractures were observed in all three boreholes, whereas horizontal fractures could not be distinguished from fracturing caused by the coring.

As described previously, the highest PCE concentration was observed in soft limestone collected at the bottom end of a core with a very high core-recovery. The next, deeper, core had a very low recovery mainly consisting of chert nodules, and no limestone samples could be obtained from this core. The FACT™ results show an abrupt decrease in PCE concentration at a depth corresponding to the interface between the two cores and a zone of low concentrations below this. The two cores were separated by a layer of chert which may have acted as a barrier to downward migration of PCE DNAPL. The other limestone sample with very high PCE concentrations was one of just three samples collected from a core with significant core loss and with high chert content (chert layer). Hence, high concentrations seem to occur in limestone above or between chert layers. The FACT™ reveals a zone at the deep end of the core interval with low concentrations, consistent with the presence of a chert layer. Several other of the concentration peaks on the FACT™ were followed by intervals with low concentrations, which suggests that the low concentration intervals are associated with chert or hard limestone and that high concentration peaks are associated with softer limestone or horizontal fractures at the interface to the harder limestone and chert. Further discussion follows in a later section.

For selected AC strips, split lengthwise, one half was initially analyzed as high resolution samples (2-10 cm each) and the other half stored and later analyzed as one long 30 cm sample to evaluate sample durability and the high resolution sampling intervals. The concentrations on the 30 cm AC samples corresponded well to the average concentration of the smaller 2-10 cm length samples from the same FACT™ interval. Hence, it is possible to store AC lengths wrapped in aluminum foil and Rilsan® bags for subsequent analysis. Average concentrations were calculated for every 30 cm section of AC from the measured high resolution AC sub-sample concentrations. In the instances where the high resolution samples revealed narrow high concentration peaks, the average concentration over 30 cm lengths was sufficiently high to allow the identification of 30 cm strips for subsequent high resolution subsampling. In this paper some depths were not analyzed. Future users of the FACT™ might consider sampling the entire length of the FACT™ and analyzing longer samples first in order to identify sections for subsequent higher resolution subsampling.

Hydraulic Conductivity Distribution in the Limestone Aquifer

The hydraulic conductivity distribution for borehole C1-C3 is shown in Figure 3. Hydraulic profiling was started at 9 m bgs and so the hydraulic conductivity for the upper 1.5-2 m of the limestone is unknown.

There is clearly a very big variation in the conductivity over depth in all three boreholes and also significant differences between the boreholes. However, all three boreholes exhibit a zone with high hydraulic conductivity (>10^{-4} m/s averaged over 0.32 m intervals, at C2 up to 10^{-3} m/s) between 9 and 11.5 m bgs., which appears to be associated with soft limestone or fractures in the vicinity of chert layers (in the upper part 9-10 m bgs.). At both C2 and C3 a high hydraulic conductivity peak (2-5·10^{-4} m/s) was observed at 19.1-19.2 m bgs. In both boreholes vertical fractures were observed in the cores at that depth. At C1 hydraulic profiling was discontinued ~18 m bgs., as the borehole was blocked by material which had dislodged from the open borehole walls during/after the drill-casing withdrawal.

All three boreholes had some zones with intermediate (10^{-5} to 10^{-4} m/s) and low conductivities (10^{-6} to 10^{-5} m/s), and single point(s) with very low (<10^{-6} m/s) hydraulic conductivities between the upper zone and the deep high hydraulic conductivity peak (19.1-19.2 m

This is a Post Print of the article published online April 6th, 2016 in Journal of Contaminant Hydrology 189 (2016) 68–85. The publishers' version is available at the permanent link: http://dx.doi.org/10.1016/j.jconhyd.2016.03.007

bgs). However, the zones of intermediate and low conductivity did not seem to be correlated between the boreholes, see details in Figure 3. In borehole C1 the zone of intermediate hydraulic conductivity dominated, whereas intermediate and low hydraulic conductivities appear evenly distributed at C2 and C3 .

The lack of correlation of the hydraulic conductivities between the boreholes over much of the depth is expected for a bryozoan limestone where bank deposition occurred. The conductivity correlation observed in the upper depths (9-11 m bgs.) may be an indication of the location of the hardground separating the middle and upper bryozoan bank complexes. All three boreholes had a relatively wide zone (1-2 m) in the upper part of the borehole where hydraulic conductivity could not be measured due to widening of the borehole (reduced liner velocity) - likely due to some collapse of the borehole wall (Figure 3), and smaller zones at greater but different depths. Not surprisingly, there appears to be some correlation between zones with core loss (figure 2) and zones with borehole wall collapse.

The flow in the limestone is expected to predominantly occur in fractures and the soft zones adjacent to chert layers (Madsen 2003). The observations reported above are consistent with this. Bulk hydraulic conductivities for the aquifer determined by pumping tests have previously been reported to range between $0.39 \cdot 10^{-4}$ (deeper section) and $4.8 \cdot 10^{-4}$ m/s (upper section) (Københavns Amt 2002). This shows that the highest conductivity zones dominate the bulk hydraulic conductivity determined by pump tests, whereas the hydraulic conductivities for individual intervals (~30 cm) are often lower. Use of the bulk hydraulic conductivities from pumping tests in prognostic tools will lead to an incorrect approximation of the flow field and plume spreading.

This is a Post Print of the article published online April 6th, 2016 in Journal of Contaminant Hydrology 189 (2016) 68–85. The publishers' version is available at the permanent link: http://dx.doi.org/10.1016/j.jconhyd.2016.03.007

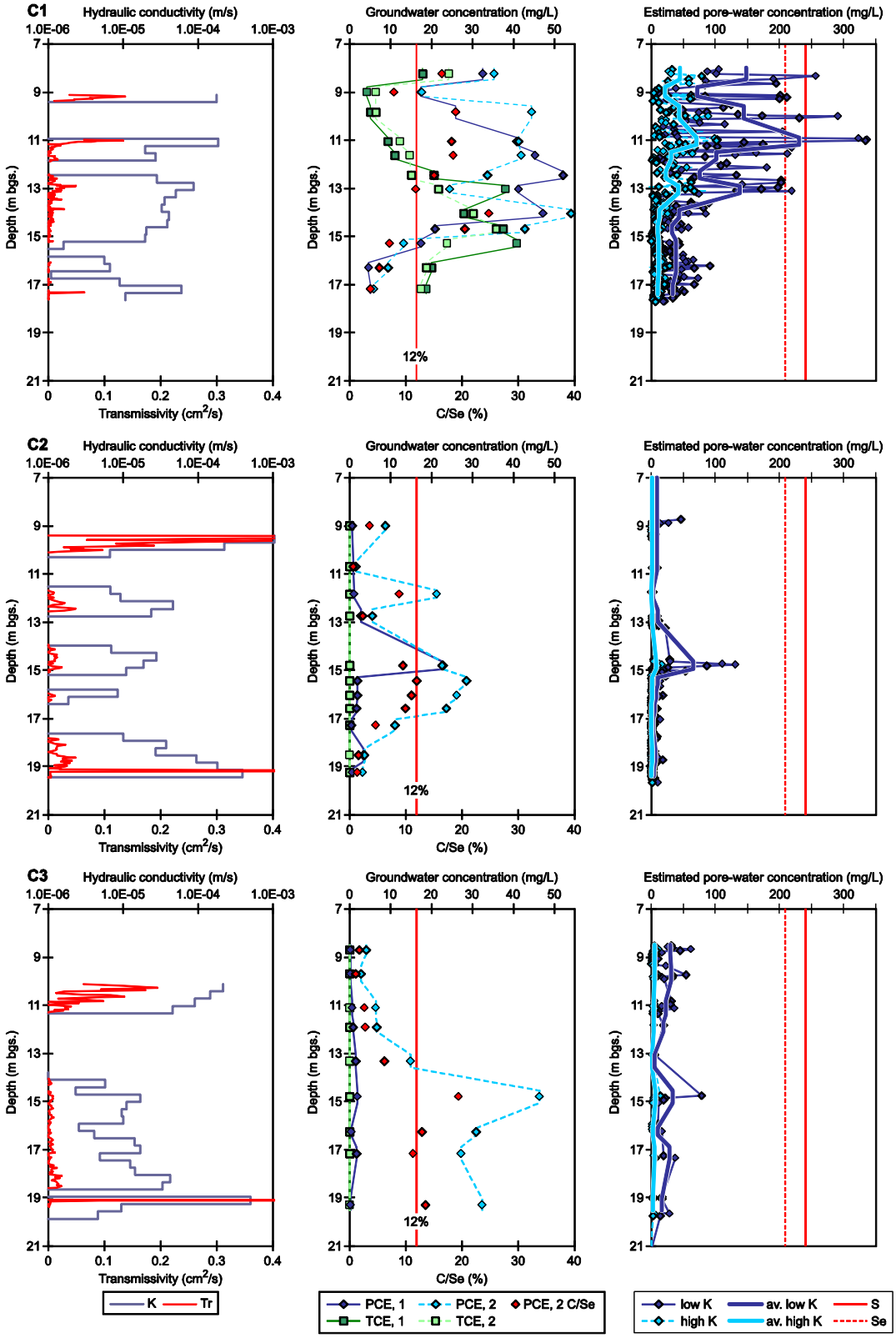

Figure 3. Limestone hydraulic parameters, groundwater concentrations (sampling event 1 (pumping on) and sampling event 2 (pumping off)) and pore-water concentrations estimated with model from FACT^{TM} concentrations for low hydraulic conductivity (diffusion controlled, low K) and for high

This is a Post Print of the article published online April 6th, 2016 in Journal of Contaminant Hydrology 189 (2016) 68–85. The publishers' version is available at the permanent link: http://dx.doi.org/10.1016/j.jconhyd.2016.03.007

hydraulic conductivity (high K) for each borehole C1-C3. In zones where no transmissivity data are shown, the liner velocity was affected by borehole widening likely caused by borehole wall collapse. Note that discrete transmissivity peak height comparison over depth may be misleading near the bottom of the hole due to the small distance traversed per time step. K: hydraulic conductivity, Tr: transmissivity, C: concentration, S: solubility, Se: effective solubility, av.: average.

Modeled Effects of Exposure and Limestone Characteristics on Uptake on FACT™

The uptake of PCE on a FACT™ when exposed to a contaminated limestone aquifer was simulated with the model and the parameters given in Table 2. After emplacement, the contaminant starts to diffuse from the aquifer into the FACT™, leading to a decreasing concentration in the aquifer close to the FACT™. The simulations indicate that diffusion is the dominating transport mechanism for the contaminant from the matrix close to the borehole into the low-conductive compressed FACT™. The transport and sorption of contaminant in the FACT™ decreases gradually with the decrease in the concentration gradient, leading to a decrease in the contaminant flux into the activated carbon strip (FACT™). At the same time, advective transport with the groundwater flow can deliver new contaminant to the borehole, thereby enhancing the contaminant flux into the FACT™. Advection can greatly increase the transport of contaminant to the FACT™, especially when highly conductive zones or fractures with strong flow intersect the FACT™ (see Figure 5b),

Figure 4 illustrates the depletion of PCE in the aquifer in the vicinity of the FACT™, the slow accumulation on the FACT™, and the steep concentration gradients in both the aquifer and the FACT™ resulting from the extremely strong sorption of PCE to AC. Figure 5a shows the slowing increase in concentrations on the FACT™ with exposure time over a 10 day period for a limestone hydraulic conductivity of 10^{-5} m/s.

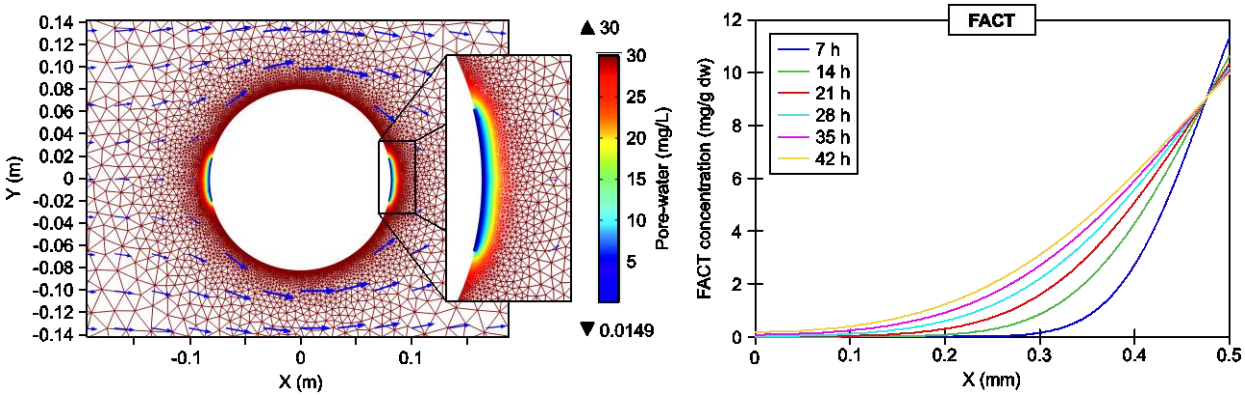

Figure 4. Porewater concentrations within the FACT after 42 hour exposure (left) and FACT™ concentrations (sorbed PCE) for different exposure durations (right).

Contaminant uptake is strongly dependent on the exposure time and hydraulic conductivity (related to the contaminant transport velocity) of the aquifer. It is also influenced by the positioning of AC-felt on the FLUTe® relative to the groundwater flow direction, the limestone matrix porosity and sorption, and AC-felt compaction (porosity) against the borehole wall. The influence of these parameters on the uptake on the FACT™ was analyzed with the model by individually varying the

This is a Post Print of the article published online April 6th, 2016 in Journal of Contaminant Hydrology 189 (2016) 68–85. The publishers' version is available at the permanent link: http://dx.doi.org/10.1016/j.jconhyd.2016.03.007

parameters as shown in Table 2. Effects of exposure time and hydraulic conductivity on the uptake on FACT^{TM} are illustrated in Figure 6A-B. The other parameters have more moderate effects (within a factor of 2 for typical parameter ranges in limestone/FACT^{TM}) and these are shown in the SM Figure S7.

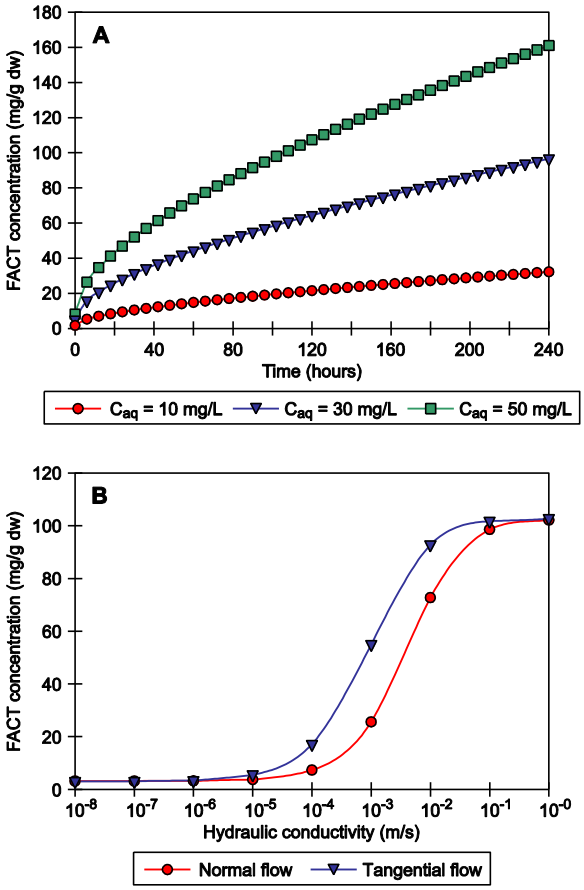

Figure 5. FACT^{TM} concentration as function of exposure time and pore water concentration for A) diffusion-dominated conditions and B) as a function of hydraulic conductivity and background flow direction after 42 hours of exposure.

With higher hydraulic conductivities the uptake increases dramatically, as shown in Figure 5B (2 orders of magnitude increase for an increase in hydraulic conductivity of 2-4 orders of magnitude for 42 hour exposure). For hydraulic conductivities >10^{-2} to10^{-1} m/s the FACT^{TM} uptake levels off because of diffusion limitations within the FACT^{TM}. Note that the results shown in the figure are dependent on the other variables, particularly the exposure time.

A series of simulation runs provided a set of linear relationships between the initial aquifer concentration and sorbed concentration for various aquifer parameters and exposure times. The linear relations were set up in a parameter dependent EXCEL spreadsheet tool, which can be exploited to convert measured sorbed concentrations on a FACT^{TM} to the aqueous aquifer concentrations in the close vicinity of the FACT^{TM}. Figure 3 (far right column) shows the conversion of the measured FACT^{TM} concentrations in the boreholes C1-C3 to porewater

This is a Post Print of the article published online April 6th, 2016 in Journal of Contaminant Hydrology 189 (2016) 68–85. The publishers' version is available at the permanent link: http://dx.doi.org/10.1016/j.jconhyd.2016.03.007

concentrations based on model simulations. The highest conductivities (high flow zones, potentially representing fractures) and the lowest conductivities (zones with very little flow, representing the limestone matrix) observed in the borehole (left column) were used for the conversion.

Chlorinated Solvent Concentrations in Groundwater Samples

The concentrations of PCE and TCE in water samples collected (sampling event 1) from the Water FLUTe^{TM} multilevel samplers installed at C1-C3 during normal operation of remedial pumping in nearby well (K11, screened 8.5-18 m bgs., pump-rate up to 5 m^3/h), and after ~3 weeks where the pump had been stopped (sampling event 2), are shown in Figure 3. Monitored pressure profiles for the multilevels during the period are shown in SM Figure S4.

The observed pressure response at C1-C3 depends on the distance to the remediation well and on the hydraulic conductivity profiles. The remediation well had the greatest effect on the pressure profile at C1, especially for the top four screened levels (8-12 m bgs.) and the deepest screened interval (~18 m bgs.), where the heads were significantly lower relative to heads at the other screened depths during remedial pumping. The change on the pressure distribution due to changes in remediation pumping was similar, but smaller at C2. At C3 changes in pumping made little difference, and the largest effect was observed in the deepest screened interval (18-20 m bgs.). For all the wells, remedial pumping had the greatest effect on the flow in the upper zone of the limestone. Core loss data suggests that the upper limestone is highly fractured/crushed, with soft limestone and chert layers. The remedial pumping also appeared to have an effect on the flow in a high conductivity zone at >18 m bgs.

The larger changes in pressure induced by the remedial pumping at some depths compared to others shows that a good seal of the Water FLUTe^{TM} liner against the borehole wall was achieved between these depths. Even in the zone 9.5-11 m bgs. where borehole collapse occurred, concentrations of samples from adjacent ports are different indicating a good seal between these depths.

The aqueous concentrations of PCE and TCE in the multilevel sampling ports in all three boreholes (C1-C3) were generally high (mg/L level) and generally exceeded 1% of the effective solubility for the PCE and TCE mixture, indicating that DNAPL presence at the site is likely. At depths up to 15m bgs at C1, PCE concentrations exceeded 10% of the absolute solubility (24 mg/L) or 12% of the effective solubility of a PCE and TCE mixture at 8 of 12 sampling ports in both sampling campaigns. The sampling ports screened over intervals where core samples contained the highest PCE content showed aqueous PCE concentrations corresponding to 10% of the absolute solubility (or 12% of effective).

The overall concentration levels at C1 were not affected by remedial pumping, though concentrations increased in some ports and decreased for others. The largest decrease in concentration was observed between 12.5 and 13 m bgs. and the largest increases around 10 and 15 m bgs. The very high concentration levels and limited effect of a pump-stop on concentrations is an indication of current or recent DNAPL presence in the limestone aquifer.

TCE concentrations were higher than PCE concentrations at C2 and C3, but PCE was highest relative to the compound solubility at both locations. The effective solubility for the PCE and TCE mixture was similar to C1. In sampling event 1 (during remedial pumping in K11) only 1 port at C2 (~14.8 m bgs.) and no ports at C3 had PCE concentrations that approached 10% of absolute PCE solubility (or 12% of effective solubility for PCE and TCE mixture). A high concentration peak was observed on the FACT^{TM} at C2 at the same depth (14.7-14.9 m bgs., 9-14 mg/g dw). At C2 at 12 m bgs. (1 point) and between 14 and 17 m bgs. (5 points), PCE concentrations increased to the same level as the 14.8 m bgs. point in sampling event 2. The observations at 14.8 m bgs. at C2 were similar to those of C1 and indicate current or recent presence

This is a Post Print of the article published online April 6th, 2016 in Journal of Contaminant Hydrology 189 (2016) 68–85. The publishers' version is available at the permanent link: http://dx.doi.org/10.1016/j.jconhyd.2016.03.007

of DNAPL in the aquifer. At 12 and 14-17 m bgs. data indicates back diffusion from a highly contaminated limestone matrix suggesting an earlier presence of DNAPL has dissolved and diffused into the matrix. The highest concentration at C3 was observed at 14 m bgs. in sampling event 1 and one port deeper in sampling event 2, where it approached the 10% of solubility level. The increase in sampling event 2 suggests that DNAPL may have been present at this depth in the past.

Method Comparison of Limestone Coring, FACT™ and Groundwater Sampling

Estimation of chlorinated solvent concentrations in porewater

The modeled porewater concentrations based on the measured concentrations of the FACT™ samples for selected hydraulic conductivities and an exposure time of 42 hours are shown in Figure 3 together with the hydraulic conductivities determined by the hydraulic profiling with the FLUTe® and concentrations in samples from the Water FLUTe™ multilevel samplers. The cyan diamonds represent pore water concentrations determined from individual FACT™ measurements and the highest hydraulic conductivities observed in each profile, and the cyan lines are averaged values calculated from the points over lengths corresponding to the lengths of the screened interval of the multilevel sampling ports (30-50 cm). Similar results are presented in dark blue for the lowest measured values of hydraulic conductivity, where the uptake on the FACT™ is diffusion-controlled.

At C1 the maximum modeled average porewater concentration and several individual point concentrations reach or exceed the aqueous solubility of PCE (240 mg/L) and the effective aqueous solubility of PCE in the mixed PCE and TCE DNAPL (~200 mg/L based on the composition in water samples from the same depth interval). Concentrations of FACT™ samples corresponding to the solubility limit are only possible if the hydraulic conductivity exceeds 10^{-5} m/s or if DNAPL is present in the vicinity of the borehole so that the concentration gradient in the porewater is and stay steep due to DNAPL dissolution. The highest hydraulic conductivity was observed in the well around 11 m bgs. ($2 \cdot 10^{-4}$ m/s). Between 8.4 and 13.3 m there are several concentration peaks where porewater concentrations estimated from FACT™ concentrations for diffusion dominated transport exceed the effective solubility for PCE. The highest of these peaks coincides with a high hydraulic conductivity zone. The two next highest are located in a zone where the hydraulic conductivity could not be measured, but may be high as it is likely a highly fractured zone. However, even for the highest hydraulic conductivity measured, the concentration is within a factor of 2 of the effective solubility. This strongly suggests that DNAPL is or has recently been present in the vicinity of borehole C1 in fractures in the depth interval 8.4-13.3 m bgs. This corresponds well with the high concentration levels in groundwater samples from the Water FLUTe™ and the highest limestone sample concentrations. We also know that the clayey till above the limestone has been compromised and that DNAPL is present in the transition zone between the clayey till and the intact limestone at CT2 only 3-4 m from C1 (Fjordbøge et al., 2016). Generally, the limestone cores had significantly lower concentration levels in the 9-13 m bgs. interval. This suggests that there was a significant loss of contaminant during collection and/or subsampling of limestone cores. This may be due to core loss in that section consistent with the likely collapse of the borehole wall as indicated by the widening of the borehole revealed by the transmissivity profiling (decreased liner velocity).

For the two deeper multilevel sampling ports in C1, aqueous PCE concentrations were high in the second sampling event (~14 m bgs. and ~15 m bgs.) and in the first sampling event (~14 m bgs.) suggesting DNAPL presence in a fracture. However, the maximum PCE concentrations on the FACT™ were lower, resulting in lower estimated porewater concentrations. When making these comparisons, it is important to keep in mind that the results may easily vary by a factor of 2-3 because of uncertainties in the parameter range for the limestone and FACT™. It is also important

This is a Post Print of the article published online April 6th, 2016 in Journal of Contaminant Hydrology 189 (2016) 68–85. The publishers' version is available at the permanent link: http://dx.doi.org/10.1016/j.jconhyd.2016.03.007

to note that for diffusion-controlled uptake over a period of 42 hours, the FACT™ only samples a zone of a width of 1 cm or less from the borehole circumference. Longer deployment/exposure times are recommended for future use in saturated limestone. For conditions similar to the studied limestone aquifer (flow, sorption capacity, etc) the sorption capacity of the AC is not likely to be exceeded for a 7-10 day exposure time.

Maximum concentrations on the FACT™ observed in boreholes C2 and C3 were not nearly as high. Porewater concentrations estimated from the highest FACT™ concentration of PCE at C2 for the diffusion-controlled case corresponded to about 30% of effective solubility. The high groundwater PCE concentration at this sampling port in both sampling events and the high rebound in the surrounding section suggests that DNAPL is or was recently present at 14.8 m bgs. at C2.

Evaluation of DNAPL presence in limestone aquifer - Conceptual understanding

It remains difficult with any certainty to determine whether DNAPL is present in the limestone aquifer today, or whether DNAPL, having migrated into the limestone aquifer through fractures in the past, has completely dissolved and diffused into the limestone matrix. However, the combined characterization techniques have provided a strong line of evidence indicating that DNAPL may currently be present in the source area in the limestone aquifer.

Based on the data evaluation, it is believed to be likely that DNAPL is present in multiple horizontal fractures and possibly in a sub-vertical fracture (observed in core at 9.5-10 m bgs.) within the depth interval 8.4-13.3 m bgs. and in a horizontal fracture at ~14 m bgs. in the vicinity of borehole C1 and at 14.8 m bgs. in the vicinity of C2. Other fractures between these and at additional depths at C2 (12 and 14-17 m bgs.) and C3 (~14.8 m bgs.) may potentially have had DNAPL present in the past, which has since then dissolved and diffused into the matrix. DNAPL may also be present at some distance from the boreholes. A conceptual model for the current (or recent) DNAPL presence in the limestone aquifer is shown in SM Figure S8.

Conclusions

Wire-line coring, is the best current technique for collection of cores in limestone aquifers, but is seriously challenged by the heterogeneous geology of limestone with varying layers of very hard chert beds/nodules and soft limestone. This heterogeneity results in significant core loss, drilling induced fracturing, and loss of contaminants from the cores. As a result, it is very difficult to use these cores as a stand-alone technique for contaminant site evaluations, where information is needed on the geology and natural fracture distribution, contaminant concentrations, and DNAPL presence. Membrane interface probing and other drive point based technologies which can yield discretized data in other geologic media such as clayey till (Fjordbøge et al., 2016) are not an option in the hard limestone and chert.

Multilevel sampling of groundwater can be performed by a number of existing techniques. The Water FLUTe™ used in this study provides well discretized data (12 screened levels for each borehole) for single borehole applications and has a very low pre-purge requirement, limiting the bias due to dilution of contaminant concentrations by large purge volumes. Multilevel sampled concentrations are biased toward larger fractures and high conductivity conduits in the limestone where there is a significant flow, collecting only a small portion of samples from smaller fractures and matrix. At the test site, very high aqueous concentrations suggest current or past presence of DNAPL, but it is difficult to confirm the current presence of DNAPL from water samples. A rebound test with the multilevel sampler, where remedial pumping was temporarily discontinued, proved to be very useful in the line of evidence for DNAPL.

The FLUTe® transmissivity profiling provided valuable information on the vertical distribution of hydraulic conductivity/transmissivity in the limestone aquifer and through this on

This is a Post Print of the article published online April 6th, 2016 in Journal of Contaminant Hydrology 189 (2016) 68–85. The publishers' version is available at the permanent link: http://dx.doi.org/10.1016/j.jconhyd.2016.03.007

likely fracture locations and preferential flow conduits. Where the integrity of the borehole wall was compromised (wall collapse) the liner velocity decreased and transmissivity profiling was affected.

Finally, the FACT™ provided highly discretized data on the depth distribution of contaminant in the aquifer, revealing typical characteristics of a fracture-matrix system including processes of matrix diffusion. FACT™ measurements of concentration are sensitive to exposure time, compound competition, flow and other aquifer- and compound parameters. A longer deployment time and the use of a pump tube to remove displaced water during installation can limit the influence of disturbances from drilling and pumping activities and FACT™ installation on AC results and thereby improve the technique. A model can be used to interpret the data and provide information on likely porewater concentrations enabling the evaluation of whether DNAPL is present in the aquifer and identifying its approximate location. The combined use of transmissivity profiling, FACT™ with modeling, and the Water FLUTe™ with rebound testing can provide detailed information on DNAPL source zone architecture.

For the limestone aquifer at the test site, results indicate horizontal spreading in the upper crushed zone, vertical migration through fractures in the bryozoan limestone down to about 16-18 m depth with some horizontal migration along horizontal fractures within the limestone. Strong evidence was provided by the FACT™ and Water FLUTe™ for detecting residual DNAPL in the limestone aquifer.

Acknowledgements

The research presented was funded by the Capitol Region of Denmark through two research collaboration agreements with DTU Environment "DNAPL source area characterization techniques" and "Chlorinated solvent contaminant migration and remediation in fractured limestone aquifers". The authors acknowledge the assistance with field and laboratory work, analysis, and graphical assistance by technical staff, research assistants and MSc students at DTU Environment: Bent H. Skov, Jens S. Sørensen, Mie B. Sørensen, Torben Dolin, Monique Beyer. The assistance of technical staff and colleagues from COWI, NIRAS, FLUTe and Aarslev, during the project are also acknowledged.

References

Annable, M.D., 2008. The site characterisation challenge: providing adequate data to make site management decisions at acceptable costs. Proc. 6th International Groundwater Quality Conference (Freemantle, Western Australia, 2-7 December 2007). IAHS Publ., 2008.

Beyer, M., 2012. DNAPL characterization in clayey till and chalk by FACT. MSc thesis, Department of Environmental Engineering, Technical University of Denmark.

Black, W.H., Smith, H.R., and Patton, F.D., 1986. Multiple-level ground-water monitoring with the MP system. In *Proceedings of the Conference on Surface and Borehole Geophysical Methods and Ground Water Instrumentation*. National Water Well Association, 41-61. Dublin, Ohio. NWWA.

Broholm, K., and Feenstra, S., 1995. Laboratory measurements of the aqueous solubility of mixtures of chlorinated solvents. Environ. Toxicol. Chem., 14(1): 9-15.

Brotzen, F., 1959. On tylosidaris species (Echinoedes) and the stratigraphy of the Danian of Sweden. SGU, Ser. C, 571, 1-81.

Chambon, J., Damgaard, I., Christiansen, C., Lemming, G., Broholm, M.M., Binning, P.J., and Bjerg, P.L., 2009a. Model assessment of reductive dechlorination as a remediation technology for contaminant sources in fractured clay. Modeling tool, Delrapport II. DTU Environment, Environmental Project No. 1295, 2009, Miljøproject, 2009a.

This is a Post Print of the article published online April 6th, 2016 in Journal of Contaminant Hydrology 189 (2016) 68–85. The publishers' version is available at the permanent link: http://dx.doi.org/10.1016/j.jconhyd.2016.03.007

Chambon, J., Lemming, G., Broholm, M.M., Binning, P.J., and Bjerg, P.L., 2009b. Model assessment of reductive dechlorination as a remediation technology for contaminant sources in fractured clay. Case studies, Delrapport III. DTU Environment. Environmental Project No. 1296 2009, Miljøproject, 2009b.

Cherry, J.A., and Johnson, P., 1982. A Multilevel Device for Monitoring in Fractured Rock. *Ground Water Monitoring Review*, 2 no. 3: 41-44.

Cherry, J.A., Parker, B., and Keller, C., 2007. A new depth-discrete multilevel monitoring approach for fractured rock. *Ground Water Monitoring and Remediation* 27 no.2: 57-70.

Clausse, B., Garrot, B., Cornier, C., Paulin, C., Simonot-Grange, M.H., Boutros, F., 1998. Adsorption of chlorinated volatile organic compounds on hydrophobic faujasite: correlation between the thermodynamic and kinetic properties and the prediction of air cleaning, Microporous and Mesoporous Materials 25, pp. 169–177.

Damgaard, I., Bjerg, P.L., Jacobsen, C.S., Tsitonaki, A., Kernn-Jespersen, H., Broholm, M.M., 2013a. Performance of full scale bioremediation in clay till using enhanced reductive dechlorination. *Ground Water Monitoring & Remediation*. 33(1): 48–61.

Damgaard, I., Bjerg, P.L., Bælum, J., Scheutz, C., Hunkeler, D., Jacobsen, C.S., Tuxen, N., Broholm, M.M., 2013b. Identification of chlorinated solvents degradation zones in clay till by high resolution chemical, microbial and compound specific isotope analysis. *Journal of Contaminant Hydrology* 146: 37–50.

Damholt, T., and Surlyk, F., 2014. Stevns Klint – ny dansk verdensarv. Ed.: Gravesen, P.. Geoviden. Geologi og Geografi. 2014 Nr. 3. pp 20.

Einarson, M.D. 2006. Multilevel Ground-Water Monitoring. In *The Practical Handbook of Environmental Site Investigations and Ground-Water Monitoring*, 2. ed, chap. 11, ed. D. Nielsen, 808-848. Boca Raton, Florida. CRC Press.

Einarson, M.D., and Cherry, J.A., 2002. A New Multilevel Ground Water Monitoring System Using Multi Channel Tubing. *Ground Water Monitoring and Remediation* 22 no. 4: 52-65.

Erto, A., Lancia, A., Musmarra, D., 2011. A modelling analysis of PCE/TCE mixture adsorption based on Ideal Adsorbed Solution Theory, Separation and Purification Technology 80, pp 140–147.

Feenstra, S., Cherry, J.A., Parker, B.L., 1996. Conceptual models for the behavior of dense non-aqueous phase liquids (DNAPLs) in the subsurface, in Dense chlorinated solvents and other DNAPLs. J.F. Pankow and J.A. Cherry, eds. Waterloo Press p53-88. Portland, O.R., U.S.A.

Fjordbøge, A.S., Janniche, G.S., Jørgensen, T.H., Grosen, B., Wealthall, G., Christensen, A.G., Kerrn-Jespersen, H., and Broholm, M.M., 2016. Assessment of the integrity of clay aquitards in aquifer protection at a DNAPL release site: Use of current and emerging site characterization tools. Manuscript submitted to *Journal of Contaminant Hydrology*.

GEO and GEUS, 2014. Strømning og stoftransport i kalklagene på den københavnske vestegn. Geologisk og hydrologisk vidensopsamling og typemodel. Report for Capital Region of Denmark, pp. 87.

Geoviden, 2014. GEUS.

Goode, D.J., Imbrigiotta, T.E., Lacombe, P.J., 2014. High-resolution delineation of chlorinated volatile organic compounds in a dipping, fractured mudstone: Depth- and strata-dependent spatial variability from rock-core sampling. Journal of Contaminant Hydrology, 171, 1-11.

Gravesen, P., Ulbak, K., Jakobsen, P.R., 2010. Radon og radioaktivitet i danske bjergarter og sedimenter. 2010. Geocenter Danmark. Geoviden, Geologi og Geografi, 2010-4.

This is a Post Print of the article published online April 6th, 2016 in Journal of Contaminant Hydrology 189 (2016) 68–85. The publishers' version is available at the permanent link: http://dx.doi.org/10.1016/j.jconhyd.2016.03.007

Hewitt, A.D. 1998. Comparison of sample preparation methods for the analysis of volatile organic compounds in soil samples: Solvent extraction vs. vapor partitioning. Environmental Sciences & Technology 32, no. 1: 143–149.

Jakobsen, R., Høgh-Jensen, K., and Brettmann, K.L., 1993. Tracer Test in Fractured Chalk 1. Experimental Design and Results. *Nordic Hydrology*, 24(4),p. 263-274.

Janniche, G.S., Fjordbøge, A.S., and Broholm, M.M., 2013. DNAPL i moræneler og kalk – vurdering af undersøgelsesmetoder og konceptuel modeludvikling. Naverland 26AB, Albertslund. DTU Environment and Capital Region of Denmark (In Danish). www.sara.env.dtu.dk (accessed 10 12, 2015).

Kueper, B.H., Davies, K.L., 2009. Assessment and delineation of DNAPL source zones at hazardous waste sites. United States Environmental Protection Agency, Publication EPA/600/R-09/119.

Københavns Amt, 2002. Omfattende undersøgelser Naverland 26AB. Prepared by Orbicon.

Keller, C.E., Cherry, J.A., Parker, B.L., 2014. New Method for Continuous Transmissivity Profiling in Fractured Rock, Groundwater, 52(3), 352-367.

Lawrence, A.R., Chilton, P.J., Barron, R.J., and Thomas, W.M., 1990. A Method for Determining Volatile Organic Solvents in Chalk Pore Waters (Southern and Eastern England) and its Relevance to the evaluation of Groundwater Contamination. *Journal of Contaminant Hydrogeology* 6: 377-386.

Loop, C.M., and White, W.B., 2001. A conceptual model for DNAPL transport in karst ground water basins. *Ground Water*, 39(1), 119-127.

Madsen, P.R., 2003. Simulering af fersk/salt-vandsgrænsens stabilitet i opsprækkede kalkaflejringer - udvaskning af klorid fra opsprækket bryozokalk. MSc thesis. DTU Environment.

Mercer, J.W., Cohen, R.M., and Noel, M.R., 2010. DNAPL site characterization issues at chlorinated solvent sites. In H.F. Stroo and C.H. Ward (eds.), In Situ Remediation of Chlorinated Solvent Plumes. Springer Science+Business Media, LLC 2010.

National Academi of Sciences, Engineering and Medicine (NAS), 2015. Characterization, Modeling, Monitoring, and Remediation of Fractured Rock. Washington D.C.: The National Academies Press.

O'Connor, T.P., Mueller, J., 2001. Modeling competitive adsorption of chlorinated volatile organic compounds with the Dubinin–Radushkevich equation, Microporous and Mesoporous Materials 46, pp. 341-349.

Parker, B.L., Cherry, J.A., and Swanson, B.J., 2006. A Multilevel System for High-Resolution Monitoring in Rotasonic Boreholes. Ground Water Monitoring and Remediation 26 no. 4: 57:73.

Pedersen, S.A.S., 1988. Glacitectonite: Brecciated sediments and cataclastic sedimentary rocks formed subglacially. Genetic classification of glacigenic deposits Eds.: Goldthwait and Matsch. Balkema, Rotterdam, Netherlands, 89-91.

Pedersen, S.A.S., 2014. Architecture of glaciotectonic complexes. Geosciences, 4, 269-296.

Pedersen, L.C., Vilsgaard, K.D., 2013. Evaluering af afværgepumpning til afskæring af en forurening medklorerede opløsningsmidler i et kalkmagasin. DTU Environment.

Piwoni, M.D., and Banerjee, P., 1989. Sorption of volatile organic solvents from aqueous solution onto subsurface solids. Journal Contam. Hydrol., 4, 163-179.

Ponsin, V., Chablais, A., Dumont, J., Radakovitch, O., and Höhener, P., 2015. ^{222}Rn as Natural Tracer for LNAPL Recovery in a Crude Oil-Contaminated Aquifer. Groundwater Monitoring & Remediation, p1-9, doi: 10.1111/gwmr.12091.

This is a Post Print of the article published online April 6th, 2016 in Journal of Contaminant Hydrology 189 (2016) 68–85. The publishers' version is available at the permanent link: http://dx.doi.org/10.1016/j.jconhyd.2016.03.007

Quinn,P., Cherry, J.A., Parker, B.L., 2015. Combined use of straddle packer testing and FLUTe profiling for hydraulic testing in fractured rock boreholes. Journal of Hydrology, 524(2015), 439-454.

Salzer, J., 2013. Sorption capacity and governing parameters for chlorinated solvents in chalk aquifers. MSc-thesis, DTU Environment, Technical University of Denmark.

Semprini, L., Hopkins, O.S., and Tasker, B.R., 2000. Laboratory, field and modeling studies of radon-222 as a natural tracer for monitoring NAPL contamination. Transport in Porous Media 38: 223-240.

Semprini, L., and Istok, J., 2006. Radon-222 as a Natural Tracer for Monitoring the Remediation of NAPL Contamination in the Subsurface. The Environmental Security Technology Certification Program.

Scheutz, C., M.M. Broholm, Durant, N.D., Weeth, E.B., Jorgensen, T.H., Dennis, P., Jacobsen, C.S., Cox, E.E., Chambon, J.C., and Bjerg, P.L., 2010. Field evaluation of biological enhanced reductive dechlorination of chloroethenes in clayey till. *Environmental Science & Technology* 44, no. 13: 5134–5141.

Schubert, M., Paschke, A., Lau, S., Geyer, W., and Knoller, K., 2007. Radon as a naturally occurring tracer for the assessment of residual NAPL contamination of aquifers. Environmental Pollution, 145(3): 920-927

Stenestad, E., 1976. Københavnsområdets geologiisær baseret på citybaneundersøgelserne.Geological Survey of Denmark, 3 række 45, 1-149.

Sterling, S.N., Parker, B.L., Cherry, J.A., Williams, J.H., Lane Jr., J.W., and Haeni, F.P., 2005. Vertical Cross Contamination of Trichloroethylene in a Borehole in Fractured Sandstone. *Ground Water*, 43 no. 4, 557-573.

Surlyk, F., Damholt, T., Bjergager, M., 2006. Stevns Klint, Denmark: Uppermost Maastrichtian chalk, Cretasius-Tertiary boundary, and lower Danian bryozoan mound complex. Bulletin of the Geological Society of Denmark, vol. 54, 1-48.

Varol, O., 1998: Palaeogene. In: Bown, P.R. (Ed.), Calcareous Nannofossil Biostratigraphy. British Micropalaeontological Society Series, Chapman & Hall/Kluwer Academic, 200–224.

Williams, A., Bloomfield, J., Griffiths, K., and Butler, A., 2006. Characterising the Vertical Variations in Hydraulic Conductivity within the Chalk Aquifer. *Journal of Hydrology* 330: 53-62.

Winslow, S.D., Pepich, B.V., Martin, J.J., Hallberg, G.R., Munch, D.J., Frebis, C.P., Hedrick, E.J., Krop, R.A., 2006. Statistical procedures for determination and verification of minimum reporting levels for drinking water methods. *Environ. Sci. Technol.*, 40, 281-288.

Witthüser, K., Reichert, B., and Hötzl, H., 2003. Contaminant Transport in Fractured Chalk: Laboratory and Field Experiments. *Ground Water* 41, no. 6: 806-815.

This is a Post Print of the article published online April 6th, 2016 in Journal of Contaminant Hydrology 189 (2016) 68–85. The publishers' version is available at the permanent link: http://dx.doi.org/10.1016/j.jconhyd.2016.03.007

TABLES

Table 1. FLUTe® blank liner, FACT™ NAPL-FLUTe™ and Water FLUTe™ design/dimensions for boreholes C1-C3 at the Naverland site, Denmark.

FLUTe ®blank liner	Diameter	0.162 m		
	Circumference	0.51 m		
	Length	>20 m		
	Liner material	Urethane-coated nylon fabric		
FACT™ NAPL FLUTe™	Diameter	0.164 m		
	Length	>20 m		
	Membrane material	Perforated hydrophobic fabric with hydrophobic red and blue dye stripes (solvent soluble)		
	Number of FACT strips, relative position	2, Normal to flow		
FACT™ AC-felt	Width of FACT, Foil	0.04 ± 0.001 m, 0.05 m		
	Thickness	0.0025 ± 0.0005 m (uncompressed*)		
	Density	0.064 ± 0.003 g/cc (uncompressed*)		
Water FLUTe™	Diameter	0.162 m		
	Length	>20 m, excess wrapped over top of pre-installed casing		
	Borehole	C1	C2	C3
	Sampling intervals #	12	13	13
	Depth intervals (m bgs.)	8.00-8.50 8.80-9.20 9.60-10.10 10.90-11.20 11.50-11.80 12.30-12.60 12.90-13.20 13.90-14.20 14.55-14.85 15.15-15.45 16.10-16.50 17.00-17.40	8.80-9.20 9.60-9.90 10.50-10.90 11.70-12.00 12.48-13.00 13.85-14.33 14.65-14.95 15.30-15.60 15.90-16.20 16.45-16.75 17.05-17.50 18.25-18.80 19.10-19.40	8.50-8.90 9.40-10.00 10.80-11.40 11.72-12.10 12.40-12.70 13.05-13.60 13.90-14.20 14.55-15.05 15.50-15.80 16.10-16.40 16.90-17.40 18.05-18.35 19.05-19.53

*: When the liner is filled with water to seal it against the borehole wall, the AC-felt is compressed.

This is a Post Print of the article published online April 6th, 2016 in Journal of Contaminant Hydrology 189 (2016) 68–85. The publishers' version is available at the permanent link: http://dx.doi.org/10.1016/j.jconhyd.2016.03.007

Table 2. Overview of parameters for the Naverland site. Here, the FACT^{TM} parameters are for compressed conditions and PCE.

	Parameter	Value	Name	Source
General	d	16.4 cm	borehole diameter	this study
	t_{max}	42 h	time FACT was installed	this study
	D_m	$\tau D_0 \approx nD_0$	effective diffusion coefficient	Chambon et al. (2009a)
	D_0	0.018 m^2/yr	free diffusion coefficient of PCE in water	Chambon et al. (2009b)
	α_L	0.1m	longitudinal dispersivity	Assumed
	α_T	0.01m	transverse dispersivity	Assumed
FACT^{TM}	Dimensions	0.5 × 40 mm	compressed geometry of cross section	this study
	n	0.84	compressed porosity	deduced from compressed bulk density and crystalline density of carbon (~ 2 g/cm^3)
	K	10^{-7} m/s	FACT^{TM} hydraulic conductivity	Estimated
	k_d	12000 L/kg	linear sorption coefficient of PCE	this study
	ρ_b	0.32 g/cm^3	compressed bulk density	this study
Limestone	I	1 ‰	hydraulic head gradient	Pedersen and Vilsgaard (2013)
	n	0.4	bulk porosity	this study
	K	10^{-5} m/s	bulk hydraulic conductivity	this study
	k_d	1.13 L/kg (PCE, $c_w = k_d c_s$)	linear sorption coefficient for PCE in limestone	Salzer (2013)
	ρ_b	1.75 g/cm^3	bulk density	this study

This is a Post Print of the article published online April 6th, 2016 in Journal of Contaminant Hydrology 189 (2016) 68–85. The publishers' version is available at the permanent link: http://dx.doi.org/10.1016/j.jconhyd.2016.03.007

SUPPORTING MATERIAL

Characterization of Chlorinated Solvent Contamination in Limestone Using Innovative FLUTe® Technologies in Combination with Other Methods in a Line of Evidence Approach

Mette M. Broholm[1], Gry S. Janniche[1], Klaus Mosthaf[1], Annika Fjordbøge[1], Philip Binning[1], Anders G. Christensen[2], Bernt Grosen[3], Torben Jørgensen[3], Carl Keller[4], Gary Wealthall[5], and Henriette Kerrn-Jespersen[6]*

1: DTU Environment, Technical University of Denmark, Kgs. Lyngby, Denmark; 2: NIRAS, Allerød, Denmark; 3: COWI, Kgs. Lyngby, Denmark; 4: FLUTe Technology, 5: GeoSyntec Consultants, Guelph, Ontario, Canada; 6: Capital Region of Denmark, Hillerød, Denmark

This is a Post Print of the article published online April 6th, 2016 in Journal of Contaminant Hydrology 189 (2016) 68–85. The publishers' version is available at the permanent link: http://dx.doi.org/10.1016/j.jconhyd.2016.03.007

Site description

The Naverland site is located 10-15 km west of Copenhagen. The field site is a previous distribution facility for PCE, TCE and 1,1,1-TCA (1965-1983). It is estimated that around 5000 tons of PCE, 1700 tons of TCE and 200 tons of 1,1,1-TCA were handled in the period of operation. While TCE and 1,1,1-TCA were handled in barrels, PCE was mainly stored in a subsurface tank. Site investigations were initiated in 1996, where chlorinated solvents were detected in the area near the PCE storage tank. Later investigations showed high contaminant concentrations in the groundwater in the primary limestone aquifer and remedial pumping was initiated in 2008.

A site plan with borehole locations is shown in Figure S1.

FLUTe technologies overview

An overview of the FLUTe technologies applied at the site is given in Table S1 and illustrated in Figure S3.

FACT^{TM} and NAPL membrane Laboratory Testing

Experimental

To quantify the sorption characteristics of the FACT^{TM}, batch experiments were conducted by submerging ~0.04 g (1.5·1.5·0.25 cm^3) AC in ~300 mL of aqueous solution (solid:liquid ratio 10^{-4} g/g) of PCE, TCE, cDCE, or mixtures of these in varying concentration, and rotating them in the dark at 10˚C for various exposure times. The solid:liquid ratio was selected based on a series of initial sorption experiments at an intermediate concentration and exposure time of 1-3 days. Experiments were designed in order that the equilibrium concentration in batches with AC were 50-95% of that in controls (without AC). Infusion glass bottles with Teflon coated rubber stoppers were used for the sorption experiments. Experiments were conducted in duplicate or triplicate with corresponding controls for each concentration and compound combination. After a selected exposure time (> 7 days for equilibrium experiments) subsamples of the aqueous phase were analyzed (as for the water analysis, see below). To evaluate the potential effect of the NAPL membrane on the uptake on the AC, a time series sorption experiment was repeated, where the AC was placed behind a layer of NAPL membrane placed in the screw cap fitted with a teflon lined septum on the glass bottle.

Linear and Freundlich sorption isotherms were fitted to the AC sorption data by linear and non-linear regression, respectively, for determination of sorption coefficients.

FACT^{TM} DNAPL exposure tests were conducted by placing a NAPL membrane with a piece of AC in the screw-cap fitted with a Teflon coated septum on an infusion glass bottle. A few mL and 0.5 mL PCE DNAPL were added to the empty and water-filled bottles, respectively, which were inverted to expose the NAPL membrane and through this the AC to the DNAPL. For the water-filled bottles, the NAPL membrane and AC were exposed to the clean water before adding the DNAPL.

This is a Post Print of the article published online April 6th, 2016 in Journal of Contaminant Hydrology 189 (2016) 68–85. The publishers' version is available at the permanent link: http://dx.doi.org/10.1016/j.jconhyd.2016.03.007

NAPL membrane exposure tests. A NAPL membrane was exposed to TCE and PCE saturated water, as well as DNAPL, in the laboratory and visually inspected for staining or lack of staining.

Sorption on AC

The time to equilibrium results for PCE sorption on AC from aqueous solution are shown in SM Figure S5. More than 50% of the sorption occurs within 24 hours (~60% in 42 hours) but equilibrium was only reached after 6-7 days at the high solution to AC ratio necessary. The NAPL membrane had no apparent influence on the time to equilibrium, but a greater variation between the triplicates was observed in the experiments with the membrane. The time to equilibrium is expected to be similar or shorter for the less hydrophobic compounds TCE and cDCE.

Linear sorption isotherms for PCE, TCE and cDCE for single compounds and for a mixture of the three compounds in aqueous solution are shown in Figure S6a-c. Chlorinated ethenes are very strongly sorbed on AC and K_d values for the individual compounds were 12000 L/kg for PCE, 10000 L/kg for TCE, and 3000 L/kg for cDCE. The linear sorption isotherm for the individual compounds fit well over the concentration range tested (PCE and TCE 0.5-10 mg/L, cDCE 1.5-15 mg/L) , though a slightly improved fit could be obtained with a Freundlich isotherm (not shown). When a mixture of PCE, TCE and cDCE was tested (with equal initial concentrations), a clear competitive effect of PCE on TCE and cDCE sorption was observed at high PCE concentrations. This is consistent with findings by Erto et al. (2011), Clausse et al. (1998) and O'Connor (2001) for competitive sorption on granular activated carbon. The competitive effect caused significant non-linearity in the sorption isotherm for TCE and especially cDCE on AC. Results for the lowest equilibrium concentrations suggest the effect is small for <0.5 mg/L PCE.

AC DNAPL exposure effects

When AC was exposed to separate phase PCE (in excess) in the presence of water, a concentration of around 600 mg/g dw AC was obtained, both when there was direct contact and no contact of the AC with the DNAPL droplet. When there was no contact, equilibration took about 6 days (data not shown) due to the aqueous phase diffusion limitation for the uptake. In comparison the sorbed concentration at equilibrium with a saturated solution of PCE (solubility 240 mg/L) with a K_d of 12000 L/kg would be 2.88 g/g dw AC. Some uncertainty is associated with the analysis for separate phase PCE because MS response linearity is exceeded, even with high dilutions. However, results suggest a maximum sorption capacity for AC of around 600 mg/g dw AC. In the absence of water, a 10 times higher concentration (~6 g/g dw) was found on the AC, probably because of DNAPL trapping in the AC pores.

Water FLUTe™ Shipping, Design and Installation

The three Water FLUTes were constructed in Santa Fe, New Mexico, by FLUTe and shipped on six reels to the field site. The liner and tubing bundles were divided so that disposable plastic reels could be used to prevent the need for return shipment, reducing shipping costs. The associated installation equipment was shipped from the Albuquerque, New Mexico office.

This is a Post Print of the article published online April 6th, 2016 in Journal of Contaminant Hydrology 189 (2016) 68–85. The publishers' version is available at the permanent link: http://dx.doi.org/10.1016/j.jconhyd.2016.03.007

Since the liner and tubing bundle for each system were divided onto separate reels, the liner reel was setup first, allowing the installation of the liner to the halfway point. When reaching the halfway point, the liner was stopped from descending by tying it off to the wellhead roller/winch plate assembly (Green Machine). It was necessary to stop the liner descent so that the tubing extending from the liner sleeves (the tubes that connect to each sampling interval) could be connected to the tubing bundle. The next step was to remove the liner reel and setup the tubing bundle for connecting to the liner. The tubing bundle reel was setup ~6m away from the green machine to allow room for the connection process. A 3 m table was used in between the Green Machine and the tubing bundle reel to facilitate the connection process. Each tube was color coded and numbered on both the liner and the tubing bundle to prevent mixing the tubes up. After the connection process, the tubes and connection joints were inspected.

After the connection process was completed, the tubing bundle was wrapped in a sheath to protect the pumps, tubes, and liner. After the protective sheath was secured, the liner was disconnected from the Green Machine and the installation process continued. The Water FLUTe^{TM} everted to the bottom of the borehole with a ~5 psi of driving head. Once on the bottom, the FLUTe wellhead was installed. This involves organizing the tubing, supporting the tubing bundle weight on the tether bar, cutting the tubes to the proper length, and swaging the port fittings onto the tubes.

TABLE

This is a Post Print of the article published online April 6th, 2016 in Journal of Contaminant Hydrology 189 (2016) 68–85. The publishers' version is available at the permanent link: http://dx.doi.org/10.1016/j.jconhyd.2016.03.007

Table S1. Overview of Flexible Liner Underground Technology (FLUTe).

	Description	**Status**	**Ref.**
FLUTe® (blank liner)	Flexible liner made from urethane-coated nylon fabric and custom sized to a borehole. The cylindrical flexible liner is inverted into an open borehole and held tightly against the borehole wall by filling it with water, thereby sealing the entire borehole. The FLUTe® is retracted while lowering the water level inside.	Proven technology. Decades of experience.	/1/
NAPL FLUTe™	Permeable hydrophobic membrane with vertical hydrophobic dye stripes placed within a FLUTe. When the FLUTe is inverted into the borehole the dye-striped side of the hydrophobic membrane is pushed against the borehole wall. Contact with NAPL dissolves/smears the hydrophobic dyes and results in colored staining visible on the white inside of the membrane. The staining is recorded after retraction of the NAPL FLUTe.	Proven technology. Decades of experience. Years of experience in limestone aquifers	/2/
FLUTe Activated Carbon Technology (FACT™)	One or more strips of a felt made from activated carbon fibers (AC) sewn on to the back (white side) of the hydrophobic membrane of a NAPL FLUTe. The other side of the AC is protected by an aluminum foil to prevent contaminant loss from the felt. When the NAPL FLUTe with AC (the FACT NAPL FLUTe) is inverted into the borehole, water and contaminants penetrate through the permeable hydrophobic membrane and then sorb to the AC. Once saturated with water, contaminants continue to diffuse and sorb into the AC even when no water flow occurs.	Novel and innovative technology. Experience in clayey and sandy materials at a few sites. No previous experience with limestone aquifers.	
FLUTe transmissivity profiling	A blank liner (FLUTe) is inverted into the borehole. The liner velocity and the pressure is measured as the liner descends into the borehole allowing calculation of a transmissivity profile. Transmissivity peaks reveal the location of highly conductive fractures.	Novel and innovative. No previous experience with limestone aquifers.	/3, 4/
Water FLUTe™ (FLUTe MLS)	A multilevel water sampling device (same liner material) with many depth discrete intervals (up to 1 per 60 cm) for monitoring hydraulic head and water quality. The liner seals the entire hole with the exception of dedicated sampling intervals, where formation water can be extracted via a thin permeable mesh sandwiched between the formation and the liner. A positive gas displacement system drives sample water to the surface. The sampling ports are separated by spacers that should be at least 30 cm apart. Spacers are emplaced as the liner inverts into the borehole. Up to 15 ports can be installed in a10" ID water FLUTe.	Proven technology. Experience at many sites, many in bedrock aquifers, incl. limestone	/1/

This is a Post Print of the article published online April 6th, 2016 in Journal of Contaminant Hydrology 189 (2016) 68–85. The publishers' version is available at the permanent link: http://dx.doi.org/10.1016/j.jconhyd.2016.03.007

References: www.flut.com, /1/: Cherry et al. (2007), /2/: Mercer et al. (2010), /3/: Keller et al. (2014), /4/ Quinn et al. (2015). Photos of FLUTe® Technologies are shown in Figure S3. FLUTes® are designed for a specific borehole size, the dimensions of FLUTe blank liner, FACT NAPL FLUTeTM and Water FLUTeTM used in this study are shown in Table 1 in main paper.

This is a Post Print of the article published online April 6th, 2016 in Journal of Contaminant Hydrology 189 (2016) 68–85. The publishers' version is available at the permanent link: http://dx.doi.org/10.1016/j.jconhyd.2016.03.007

FIGURES

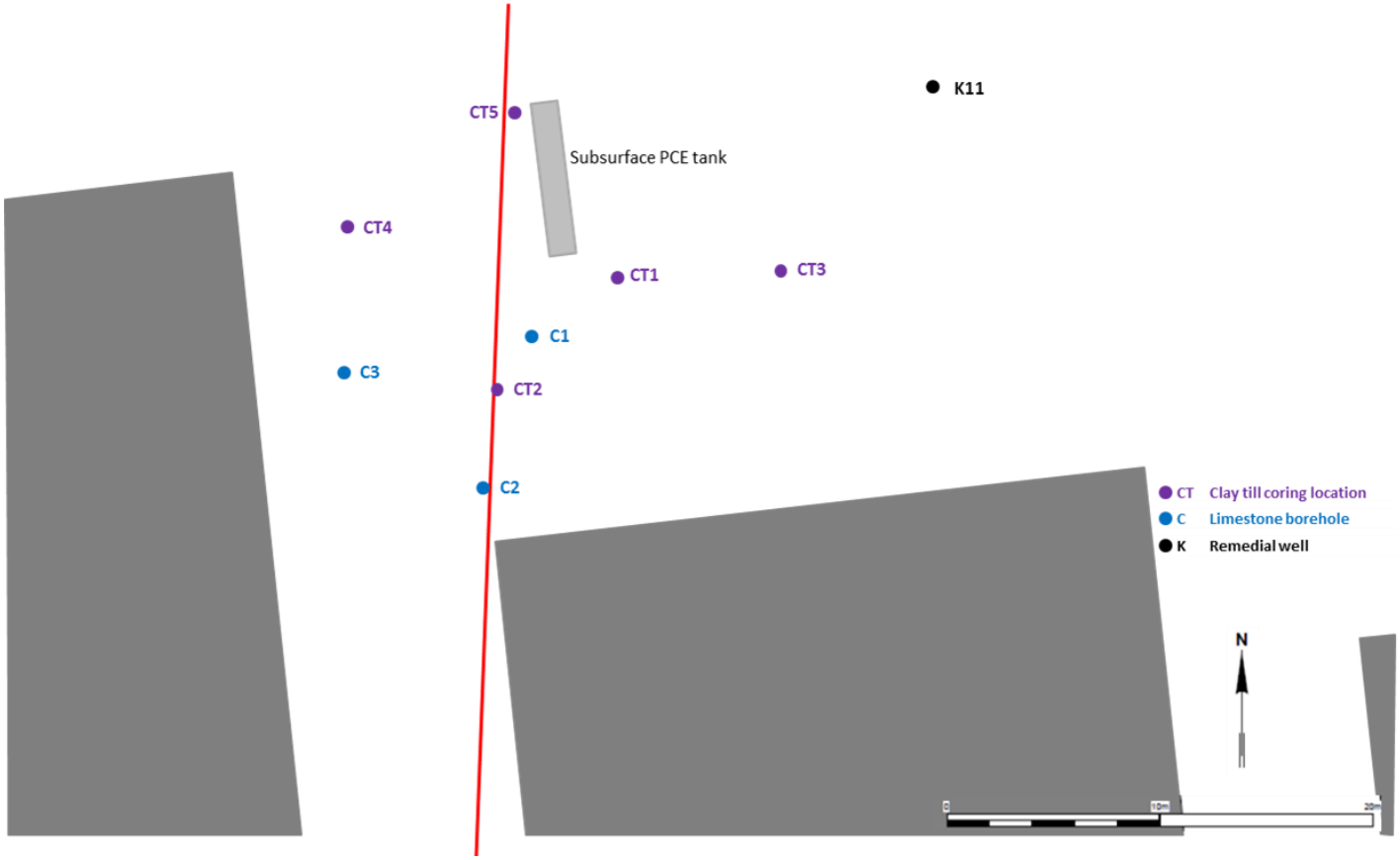

Figure S1. Overview map of the site with buildings, the previous PCE storage tank, the five clay till intact coring locations (CT1-5), the three limestone boreholes (C1-3), the remedial pumping well (K11) and the geological N-S cross section (cf. Figure S7).

This is a Post Print of the article published online April 6th, 2016 in Journal of Contaminant Hydrology 189 (2016) 68–85. The publishers' version is available at the permanent link: http://dx.doi.org/10.1016/j.jconhyd.2016.03.007

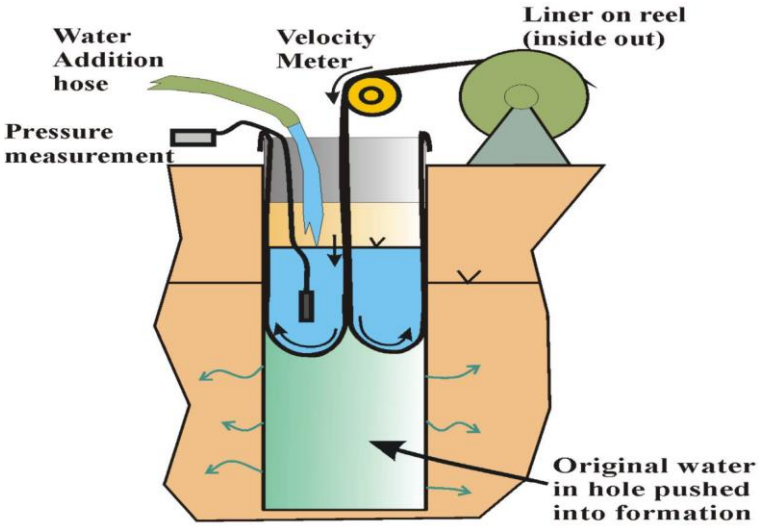

Figure S2: Transmissivity/Hydraulic profiling in borehole using FLUTe® technology. Modified from Keller et al. (2014). Provided by FLUTe®.

This is a Post Print of the article published online April 6th, 2016 in Journal of Contaminant Hydrology 189 (2016) 68–85. The publishers' version is available at the permanent link: http://dx.doi.org/10.1016/j.jconhyd.2016.03.007

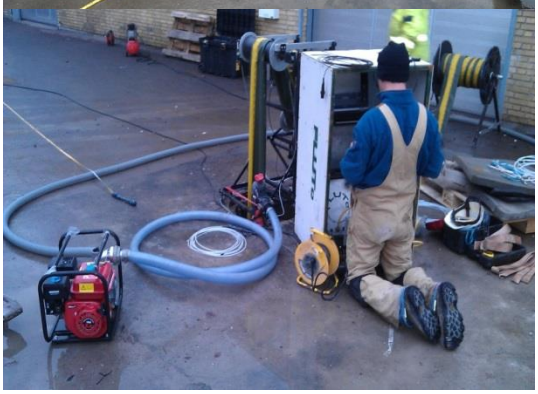

This is a Post Print of the article published online April 6th, 2016 in Journal of Contaminant Hydrology 189 (2016) 68–85. The publishers' version is available at the permanent link: http://dx.doi.org/10.1016/j.jconhyd.2016.03.007

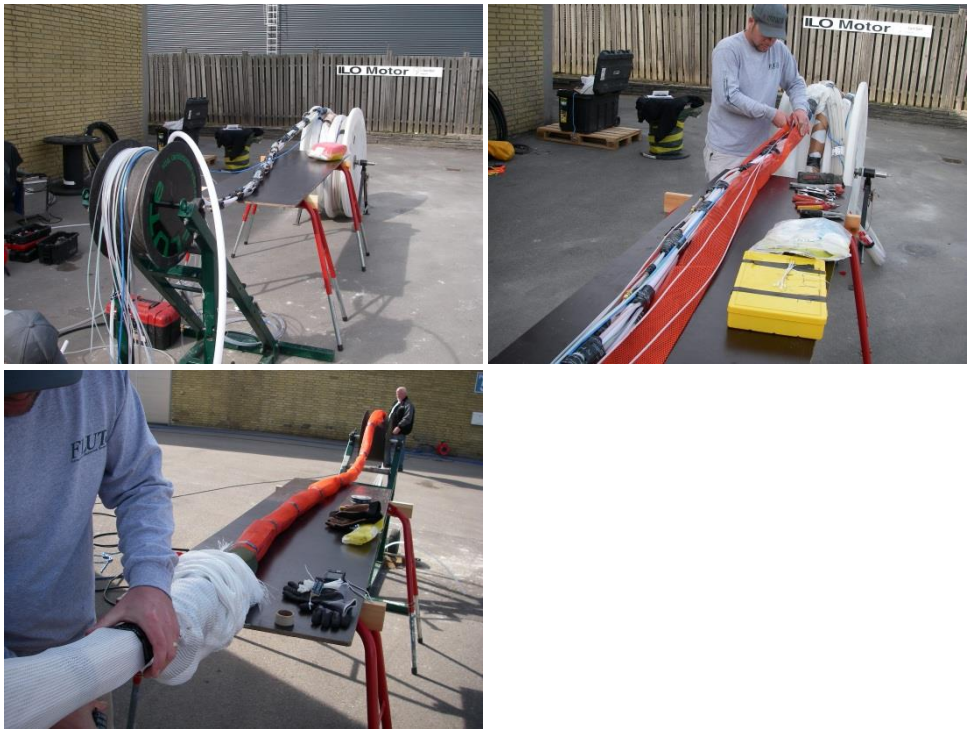

Figure S3: 1) FACT^{TM} on NAPL FLUTe^{TM}; 2) FLUTe$^{®}$ transmissivity profiling; 3) Water FLUTe^{TM} a) Inside part of Water FLUTe^{TM} sampling port, b) tubing from the sampling ports held in place in the Water FLUTe^{TM}, c) Water FLUTe^{TM} with tapering; 4) Water FLUTeTM preparation

This is a Post Print of the article published online April 6th, 2016 in Journal of Contaminant Hydrology 189 (2016) 68–85. The publishers' version is available at the permanent link: http://dx.doi.org/10.1016/j.jconhyd.2016.03.007

on site; 5) Water FLUTe™ installation a) Water FLUTe™ everted to bottom of borehole, b) FLUTe® well head, c) FLUTe® well head installation, and d) the installed water FLUTe®.

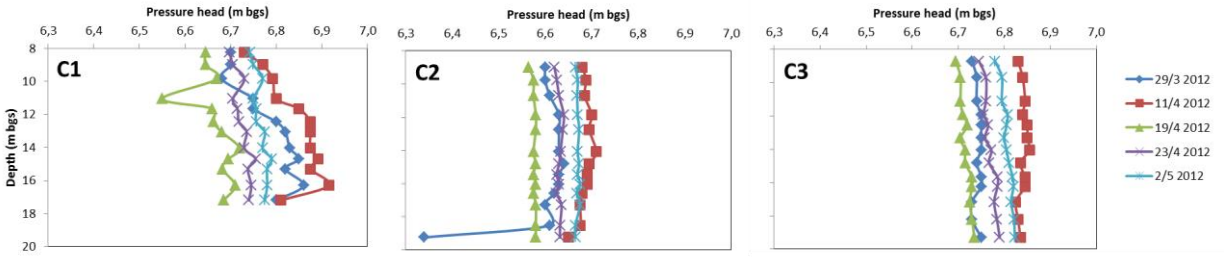

Figure S4: Pressure profile in the Water FLUTes before and during a stop of remedial pumping designed to observe contaminant rebound in aquifer.

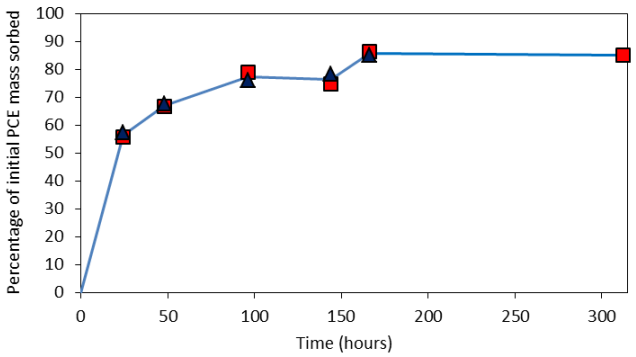

Figure S5: Time to equilibrium for sorption of PCE on FACT. Initial PCE aqueous concentration 4 mg/L, solution volume 300 mL, FACT 1.5cm by 1.5 cm, duplicate batch experiments, standard deviation for triplicate controls without FACT was 6%.

This is a Post Print of the article published online April 6, 2016 in Journal of Contaminant Hydrology 189 (2016) 68–85. The publishers' version is available at the permanent link: http://dx.doi.org/10.1016/j.jconhyd.2016.03.007

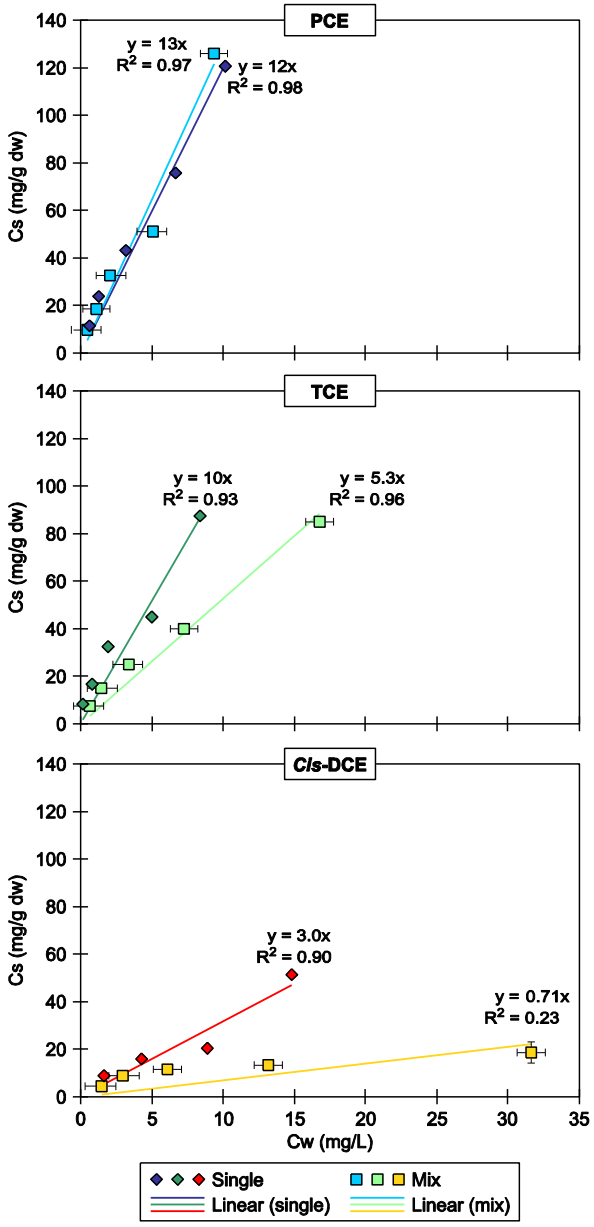

Figure S6. Sorption of individual chlorinated ethenes and a mixture of the three chlorinated ethenes in aqueous solution on AC.

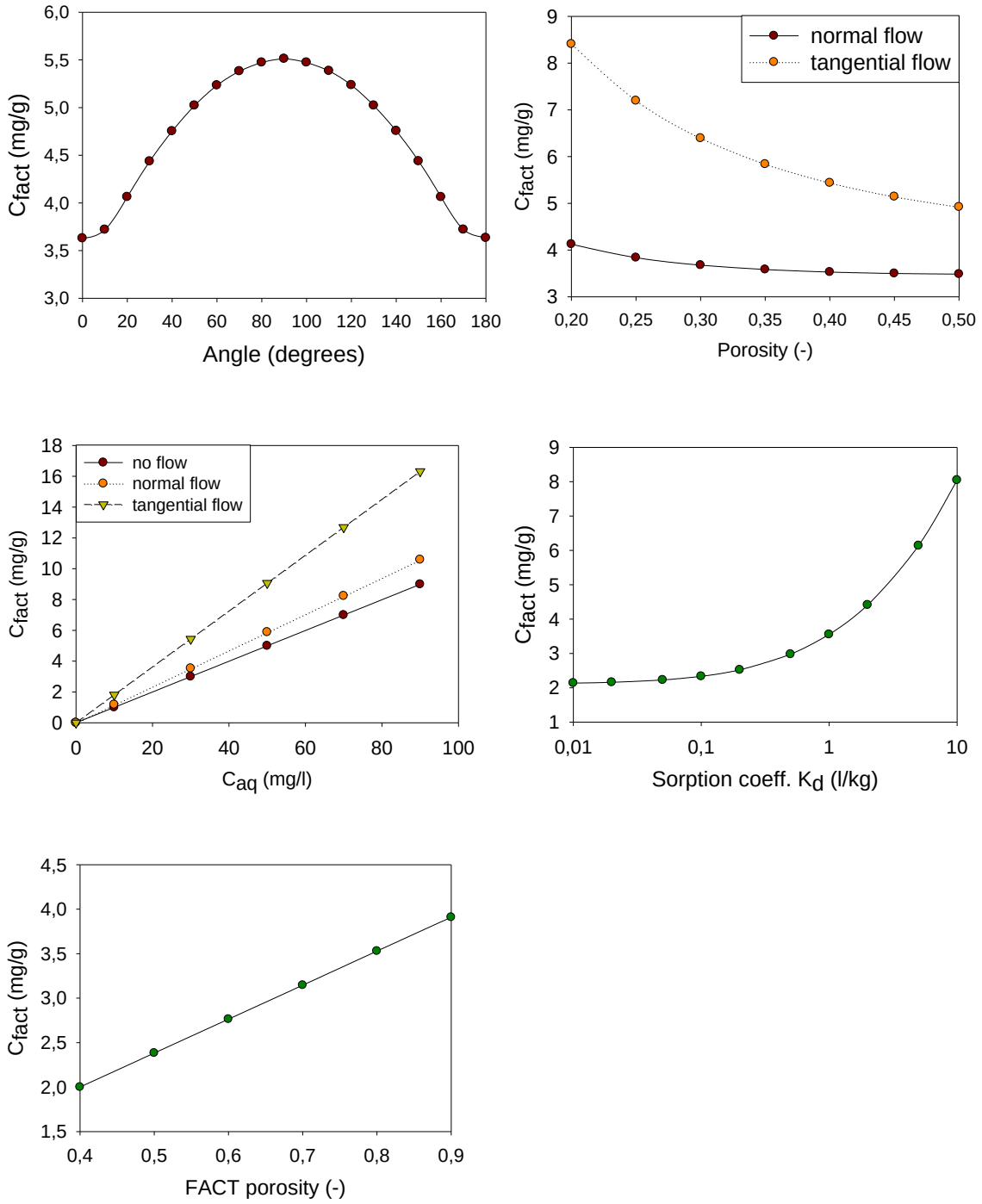

Figure S7: Modeled effects of the following parameters on uptake on FACT^{TM} from porewater under diffusion controlled conditions (from upper left to lower right): Flow angle relative to FACT^{TM}; aquifer porosity; pore-water concentration; aquifer sorption coefficient (bryozoan limestone 0.49-1.13 L/kg (Salzer 2013), calculated for low f_{oc} 0.28 L/Kg (Piwoni and Banerjee 1989); and FACT^{TM} porosity (dependent on compaction).

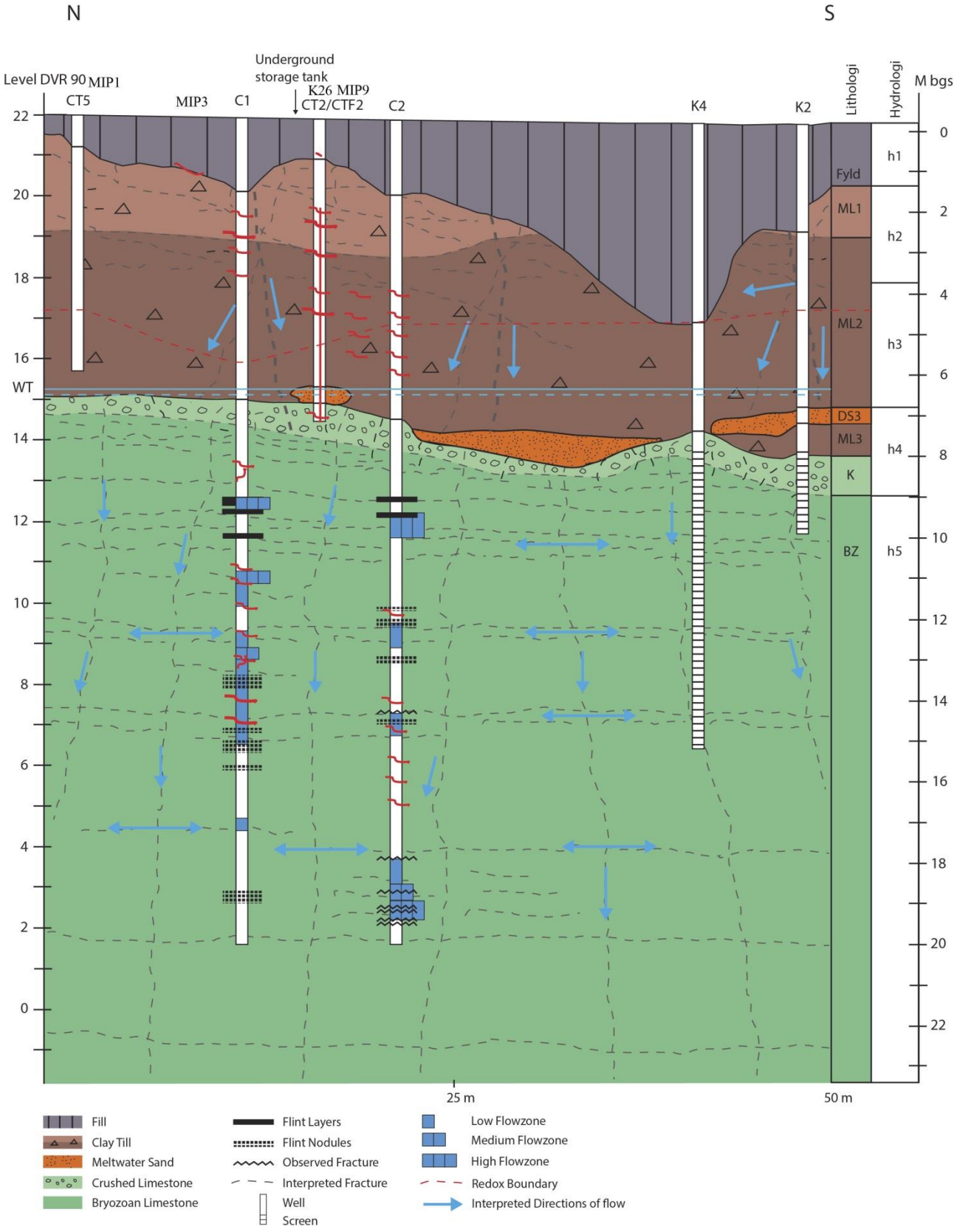

Figure S8: Conceptual model of DNAPL distribution in clayey till and limestone at the Naverland site.